Investigation of the Quench and Heating Rate Sensitivities of Selected 7000 Series Aluminum Alloys

A Thesis

Submitted to the Faculty of

WORCESTER POLYTECHNIC INSTITUTE

in partial fulfillment of the requirements for the

degree of Master of Science

In Materials Science and Engineering

by

_____
Courtney Nowill

July 2007

Approved: _____
Richard D. Sisson, Jr.
Director of Manufacturing and Materials Engineering
George F. Fuller Professor

Abstract

The quench sensitivity of AA7136 has been experimentally investigated using Jominy end quench and test coupons of various heat treatments. It was found that this alloy is not quench sensitive. In addition, the effects of heating rate on both solution and aging treatments on AA7136 and AA7075 were determined using a newly developed reverse Jominy heating test. It was observed that hardness was reduced after rapid heating during aging and hardness increased slightly after rapid heating during solutionizing. These results are discussed in terms of microstructural developments.

Acknowledgements

This project was sponsored by WPI's Center for Heat Treating Excellence.

I would like to thank my advisor Professor Richard D. Sisson, Jr. for allowing me the opportunity to work on this project and for his help, encouragement, and advice throughout this project as well as others to allow me to be where I am today.

I thank D. Scott Mackenzie of Houghton International for supplying the 7136 aluminum alloy used in this project and also for his help and suggestions. I would like to thank Dr. Mohammed Maniruzzaman for all of his invaluable assistance and suggestions throughout this study. I also thank Professor Satya Shivkumar for the identifying the potential for a reverse Jominy test, a major part of my work, and Professor Diran Apelian for being on my advisory committee. I would also like to thank Rita Shilansky for all of her time and support throughout this project.

I also would like to express my appreciation for the efforts of Torbjorn Bergstrom and Mike O'Donnell of WPI, and Thomas Kokosinski of Kokos Machine Company for their assistance.

Lastly, I thank my friends and family for all of their help to get me where I am. I especially thank my parents, Jane and Greg Nowill, for their infinite time, understanding, and support.

Worcester, MA 2007
July 2007
Courtney Nowill

Table of Contents

Executive Summary

This study investigated the effects of heating and cooling rates on two 7000 series wrought aluminum alloys, AA7136 and AA7075. There have been few studies on AA7136, an Al-Zn-Mg-Cu-Zr alloy, whereas AA7075 an Al-Zn-Mg-Cu-Cr alloy, has been studied extensively.

To determine the effects of cooling rate, a series of Jominy end quench tests, ASTM A255, were conducted where aging time and temperature was varied. Jominy end quench tests involve a bar, 2.54 cm in diameter and 10.16 cm long and water is sprayed at one end to cool the specimen, resulting in one dimensional cooling. Thermocouples placed at the center of the bar record cooling data. Properties along the bar can then be related to the cooling rate. In this study hardness was the property investigated. The Rockwell B scale was used and measurements were taken along the bar according to the standard. The hardness measurements along the AA7136 test specimens varied by less 4 HRB and the hardness measurements along the AA7075 specimens decreased by approximately 25 HRB. This data indicates that AA7136 is not quench sensitive, but AA7075 is affected by cooling rate. A series of experiments were also conducted to relate hardness to aging treatment. It was observed that peak hardness occurs at an aging treatment of 121^{o}C for 24 hours. The as-quenched hardness was 44 HRB and increased to 86 HRB after two months of natural aging at room temperature.

Optical and SEM microscopy was used to study microstructure. After solution treatment for five hours, Al-Cu-Fe particles were not dissolved, indicating that not everything was in solution. Longer treatment of 24 hours still did not dissolve the particles. An increase in temperature of 10 degrees resulted in insipient melting between grain boundaries. After aging Al-Zn-Mg-Cu precipitates were

observed in addition to the Al-Cu-Fe particles.

A test, based on Jominy end quench, was developed to study the effects of heating rate. The test apparatus is comprised of a standard Jominy bar and a KNO_3-$NaNO_3$ salt bath in a conventional furnace. The bar is placed so that one inch is submerged in the salt bath and the rest of the bar is outside the furnace. The portion of the bar outside the furnace is insulated. This results in one dimensional heating. Thermocouples were placed at the center of the bar to record heating data. Properties, hardness in this study, are then related to heating rate. Hardness measurements were taken every 3.17 mm starting from the heated end, using a Rockwell hardness tester.

The test matrix for this reverse Jominy test included experiments where the solution treatment was done using reverse Jominy followed by an aging treatment in a conventional furnace and experiments where the solution treatment was done in a conventional furnace and aging was done by reverse Jominy method. For the set of tests where reverse Jominy was conducted during solution treatment, the hardness variation was less than two and therefore, insignificant. Optical microscopy revealed fine equiaxed grains after rapid heating. Tests where the aging treatment was done by reverse Jominy resulted in a variation of 4-5 HRB at each end where the slowly heated end was harder. This is probably because the rapid heat up did not allow time for GP zones to form, where the hardening phase, $MgZn_2$, precipitates. SEM confirmed a greater density of fine precipitates after a slow quench.

Further studies should be done on both the quench sensitivity investigation and reverse Jominy testing. TEM should be used to identify the precipitates that form in AA7136 and more aging

experiments should be conducted to determine the behavior of the alloy under various conditions. For reverse Jominy, different heating methods should be investigated, such as using an oil bath so that heating rates during aging can be studied at lower temperatures, since the salt bath used in this study was not molten at temperatures below 250^{o}C. The effects of a very slow heating rate, such as less than 1^{o}C/s should be studied as well.

In conclusion, this research determined the quench sensitivity of AA7136 and the effects of heating rate on AA7136 and AA7075. AA7136 is not a quench sensitive material, but AA7075 is quench sensitive. Rapid heating rate during solution treatments results in fine equiaxed grains. Rapid heating during aging results in a lower density of precipitates and decreased mechanical properties.

Chapter I Introduction

Introduction

The 7000 series of aluminum alloys are primarily used in the aerospace industry as structural components and are strengthened by age-hardening. The 7136 wrought aluminum alloy is an Al-Zn-Mg-Cu-Zr alloy. Limited data for the aging kinetics of this particular alloy is available in the literature. A series of Jominy end-quench tests (ASTM A255) were performed to investigate the effect of cooling rate on the aging performance of the alloy. The process variables used in this study were aging time and temperature. Natural aging experiments were also conducted to verify the hardenability of the alloy at room temperature. In this study the Jominy end quench data is used to determine quench sensitivity of the alloy. The results provide a better understanding of the aging kinetics of AA7136.

Studies have shown that heating rate also has an effect on the microstructure and properties of aluminum alloys. Heating rate experiments were conducted on AA7136 and AA7075 using a salt bath and a conventional air convection furnace. In these experiments the heating rates were varied during both solution and aging treatments. With the use of a standard Jominy end quench bar a test was designed which resulted in a distribution of heating rates throughout a single specimen by means of one dimensional heating.

Chapter II
Literature Review

1. Al-Zn-Mg-Cu Alloys

The 7000 series of aluminum alloys are age-hardenable. During age-hardening, also known as precipitation hardening, precipitates form in a super saturated solid solution and strength increases as the number and size of precipitates increase until a maximum critical value is reached and the material becomes overaged and coarsening begins, reducing mechanical properties [1]. The 7000 series is made up of Al-Zn-Mg-Cu alloys where zinc is the strengthening component [2]. These alloys are primarily used in the aerospace and automotive industries because of their high strength and heat treatability. In aluminum alloys with greater than 3% Zn and a Zn to Mg ratio greater than two, the hardening mechanism is $MgZn_2$ (η) [2]. Precipitates in these alloys start as GP zones which become η′ coherent platelets and transform to η over time [3].

2. Precipitation Hardening in 7000 Series Aluminum Alloys

Precipitation hardening is affected by the chemical composition of the supersaturated solution, the composition of the phases that form during aging, the kinetics of the precipitation reactions, time, temperature, and properties of the precipitates [4]. The temperature ranges and solvus lines for heat treatment of binary aluminum alloys are shown in Figure 1.

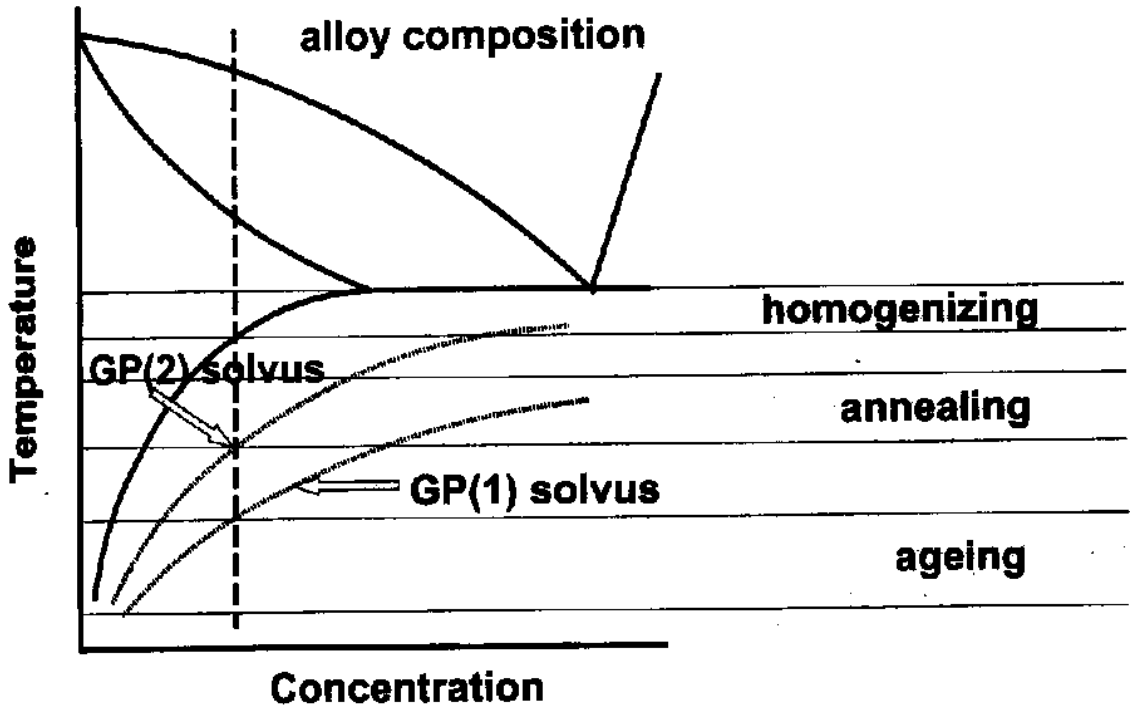

Figure 1 Temperature ranges and solvus lines for binary aluminum alloys [4]

Solution treatments are the first step in precipitation hardening. The material is heated so that there is only one phase present. In 7000 series aluminum alloys the solutionizing temperature is very close to the melting point and therefore temperature control is very important. Incipient melting may occur at grain boundaries at temperatures slightly above the solution treatment temperature where the melting point is lowest [5].

Natural aging, or aging at room temperature, occurs in most 7000 series alloys. A natural aging curve of an Al-Zn-Mg-Zr alloy is shown in Figure 2. The hardness after a water quench is observed to be greater than after a slower quench in air. In order to increase aging kinetics, artificial aging is done at a higher temperature. During natural aging the peak strength becomes stable, but in artificial aging, the strength reaches a maximum and after long aging times or high aging temperaturs the strength begins to decrease and the

alloy becomes overaged [4]. The T6 treatment, or the heat treatment that results in peak hardness, consists of a solution treatment followed by artificial aging. The common industrial artificial aging treatment for these alloys is 121C for 24 hours [6].

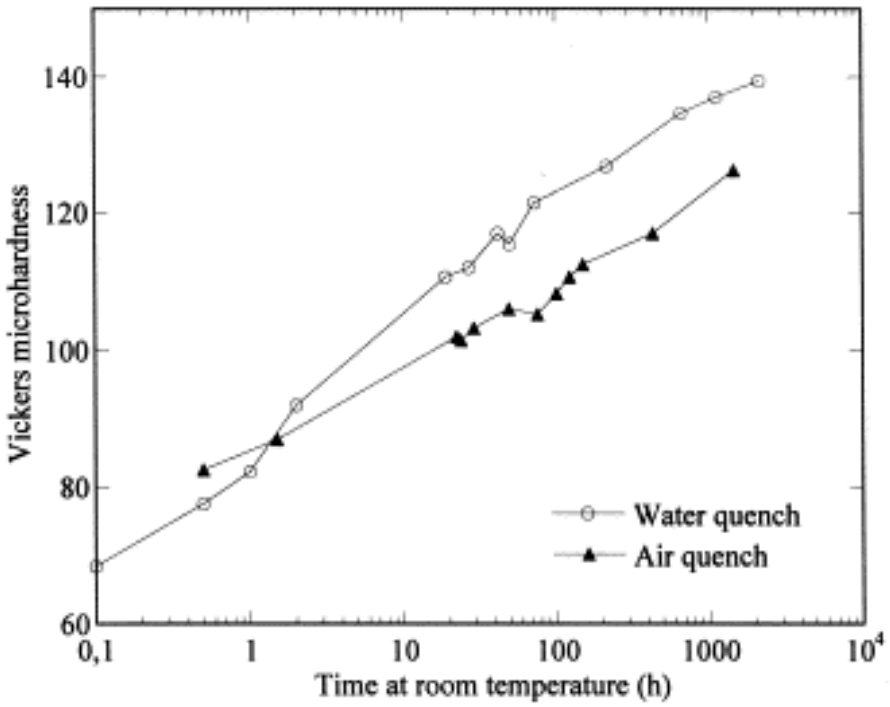

Figure 2 Natural Aging of an Al-Zn-Mg-Cu-Zr Alloy [7]

The yield strength with respect to ageing temperature and time is shown in Figure 3.

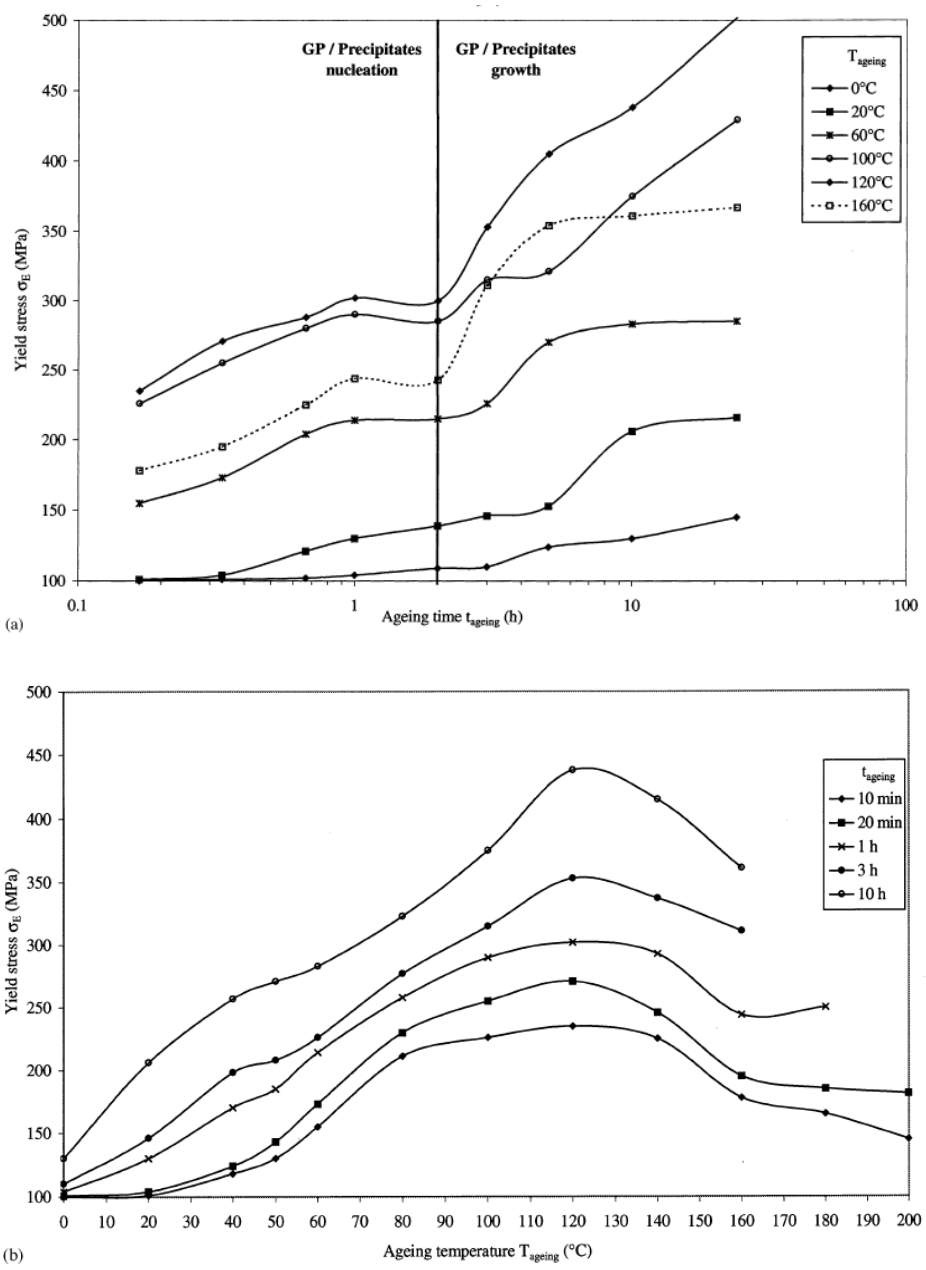

Figure 3 Yield stress versus aging (a) time and (b) temperature of an Al-Zn-Mg alloy [8]

The hardening phase, η´, results from GP zones which form on vacancy rich clusters (VRCs) from the supersaturated solution [4,9-11]. VRCs are believed to be formed right after or during a quench to room temperature [14]. The concentration of vacancies is controlled by quench rate [12,13]. Very slow quench rate in some alloys may also lead to the precipitation of coarse secondary phases [12]. Since the hardening phases rely on the

formation of GP zones and VRCs, at times, a pre-aging step is induced [10,13-15]. GP zones form between room temperature and 150^{o}C [15]. GP zones are thermally activated and need time to form [13].

These alloys can be divided into two groups: Zr containing alloys with Al_3Zr particles and Cr containing alloys with Al_7Cr particles, where Zr or Cr are added as dispersoids for grain structure control [16]. The type of dispersoid added has an effect on recrystallization kinetics as well as quench sensitivity [16,17]. Grain boundary maps of a Zr-containing alloy and a Cr-containing alloy are shown in Figure 4 [17], revealing that Cr-containing alloys have a higher fraction of recrystallization. Starink and Li [16] also showed that Zr-containing alloys are approximately 35% recrystallized and Cr-containing alloys are approximately 65% recrystallized. SEM and EDS showed that mostly S (Al_2CuMg) phase and Al_7Cu_2Fe was present in Al-Zn-Mg-Cu alloys.

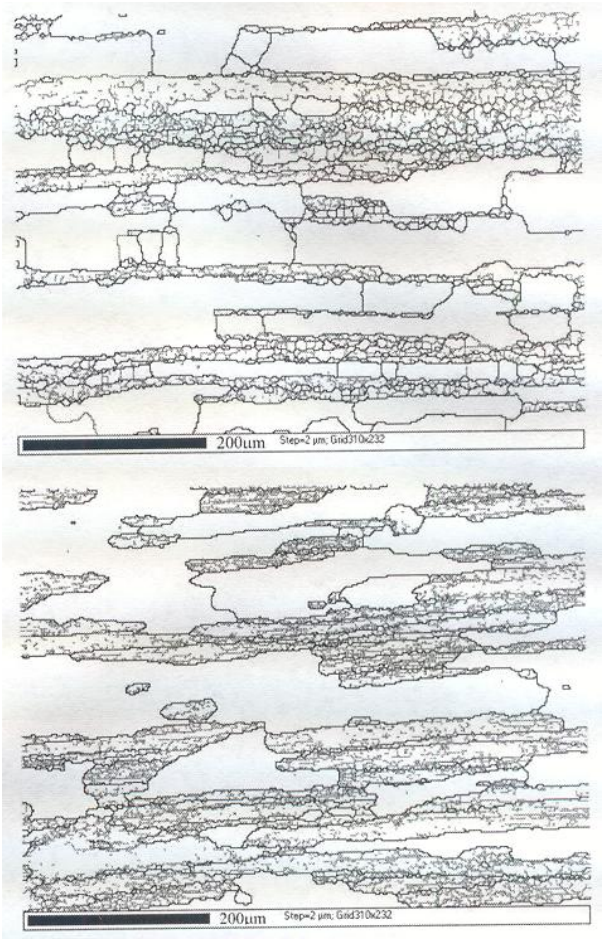

Figure 4 Grain boundary maps of (top) Zr-containing alloy and (bottom) Cr-containing alloy [17]

According to Starink and Li [16], there are three possible precipitation sequences:

(i) SSS→GP I zones→dissolution

→GP II zones→ η´→ η

(ii) SSS→T

(iii) SSS→S

where SSS is a supersaturated solid solution, GP zones are Guinier-Preston zones, η is a quaternary phase of $MgZn_2$ with AlCuMg components, T is a phase containing $Mg_3Zn_3Al_2$, and S is Al_2CuMg. The eutectic structures in 7000 alloys are αAl +

$Mg(Zn,Cu,Al)_2$ and coarse Al_7Cu_2Fe particles and a phase transformation from $Mg(Zn,Cu,Al)_2$ to Al_2CuMg occurs [18]. The dominant phase after the T6 treatment is η′. If the Zn:Mg ratio is too high then Mg_2Zn_{11}, an equilibrium phase, may also appear [19]. GP I zones tend to dissolve during heat treatment, while η′ tends to form on GP II zones [20].

The phase diagram for 8%Zn, 2%Cu, 0.3%Zr and Mg of 0-8%, a composition similar to AA7136 which is studied in this research, is shown in Figure 5.

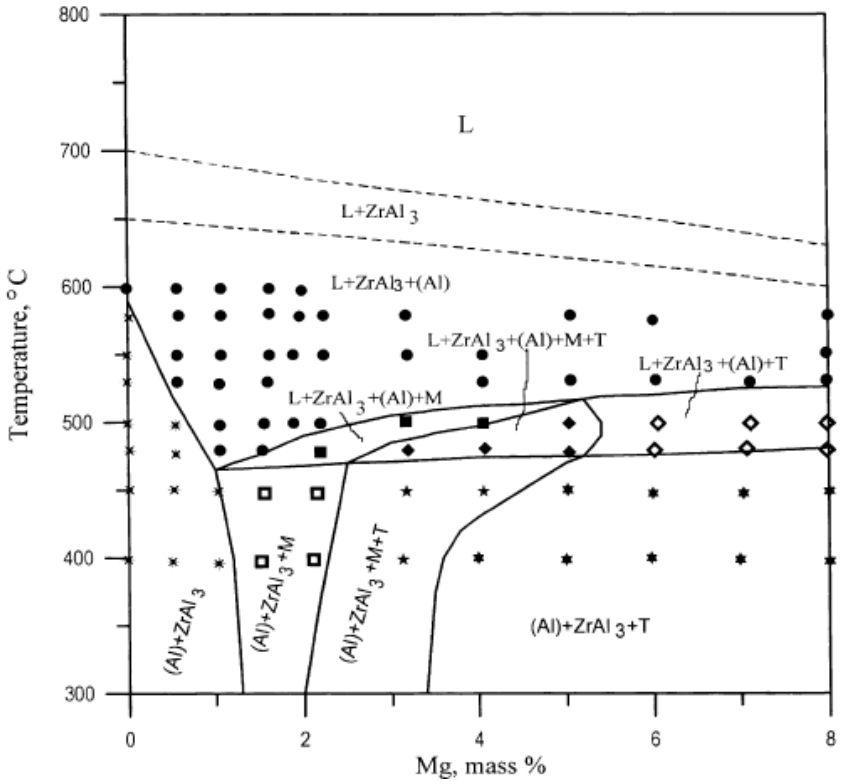

Figure 5 Calculated Phase Diagram for 8.0Zn-2.0Cu-0.3Zr-0~8.0Mg Al alloy [21]

Archambault et. al. [22] constructed a TTT curve for η precipitation shown in Figure 6.

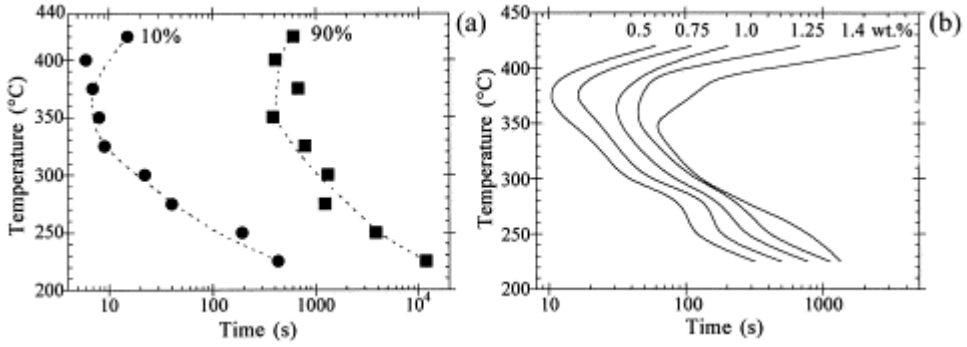

Figure 6 (a) TTT curve for η precipitation (b) Iso-precipitated weight fraction for η phase [22]

3. Quench Sensitivity

When an alloy forms non-hardenable precipitates after a slow cool, the alloy is said to be quench sensitive [23]. Alloys that experience a loss of mechanical properties due to slow cooling usually have increased electrical conductivity [13]. Quench sensitivity is important when forming thick plates, as used in the aerospace industry, because the center may be weaker than the rest of the part due to slower cooling. Figure 7 shows the cooling rate differences throughout a thick forging. Cooling rate is also important because sometimes a rapid quench may cause residual stresses in the part [24].

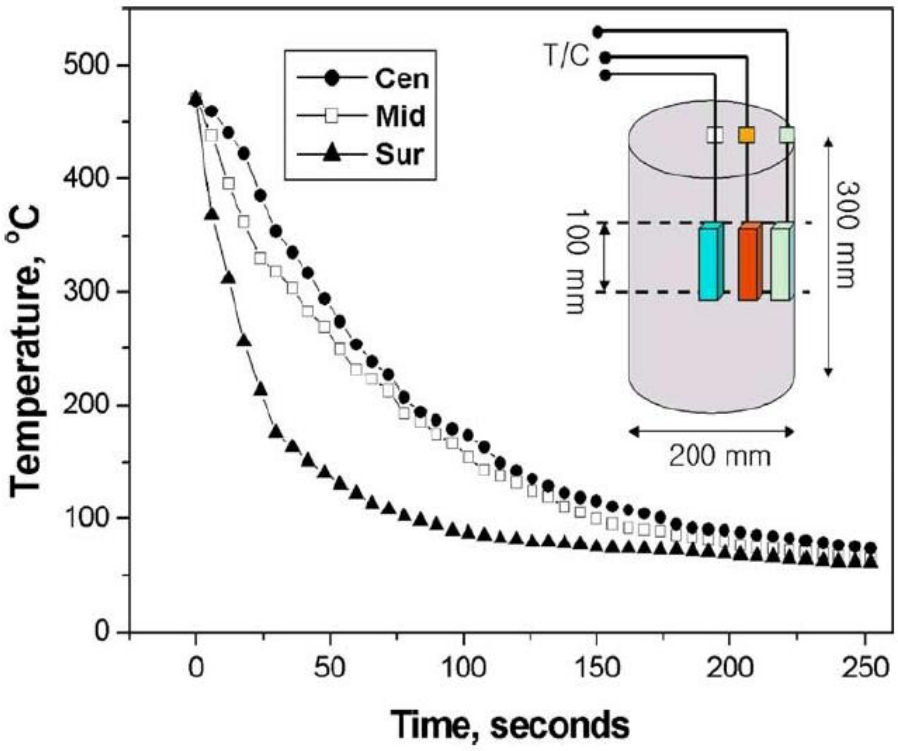

Figure 7 Cooling rate variation in a thick forging [25]

Quench sensitivity is affected by dispersoids (Zr or Cr), alloying elements (Cu, Zn and Mg), and Cu additions [16,25]. Cu has been shown to increase quench sensitivity and a higher Zn:Mg ratio allows for homogeneous nucleation and decreases quench sensitivity [16,25]. The distribution of dispersoids is dependent on the distribution of GP II zones which are not homogeneously distributed, but are in bands, due to their low diffusivity in aluminum [26]. The addition of Cu also increases the rate of precipitation in similar alloys [8]. High Zn:Mg ratios also decrease particle size and increases the precipitate number density [20]. The use of Zr over Cr dispersoids also creates a less quench sensitive material [25].

Maximum age-hardening occurs with a rapid quench since the precipitate free zone increases with quench rate [1] and heterogeneous precipitation is suppressed with faster cooling rates [24]. Although a rapid quench may result in desirable strength, thermal stresses and distortion may occur, and therefore these properties must be balanced during the cooling process [23,24]. Also, during a slow quench large precipitates may grow on dispersoids and grain boundaries, decreasing mechanical properties [13].

Jominy end quench (JEQ) experiments, ASTM A255 allow for the determination of a material's sensitivity to cooling rate [27]. The experiment, ASTM A255, uses a 25.4 mm diameter cylindrical bar which is quenched at one end, resulting in a distribution of cooling rates throughout the bar. Mechanical properties such as hardness or electrical conductivity can then be related to quench rate. Jominy end quench was first used to determine the hardenability of steels and many studies have shown that this test can be applied to nonferrous alloys as well [28-31]. Cooling rate for a 7010 Jominy end quench [24] is shown in Figure 8 with the corresponding hardness and residual stresses shown in Figure 9.

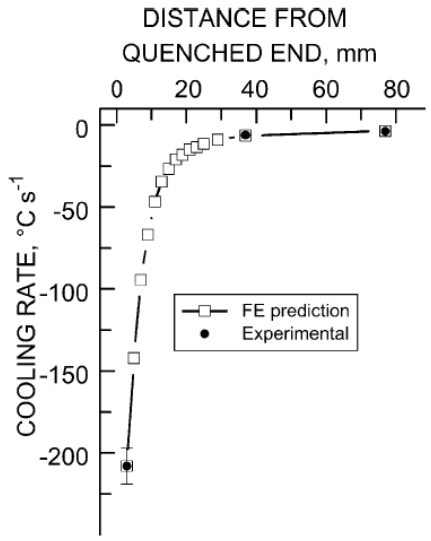

Figure 8 Cooling rate data for 7010 JEQ bar [24]

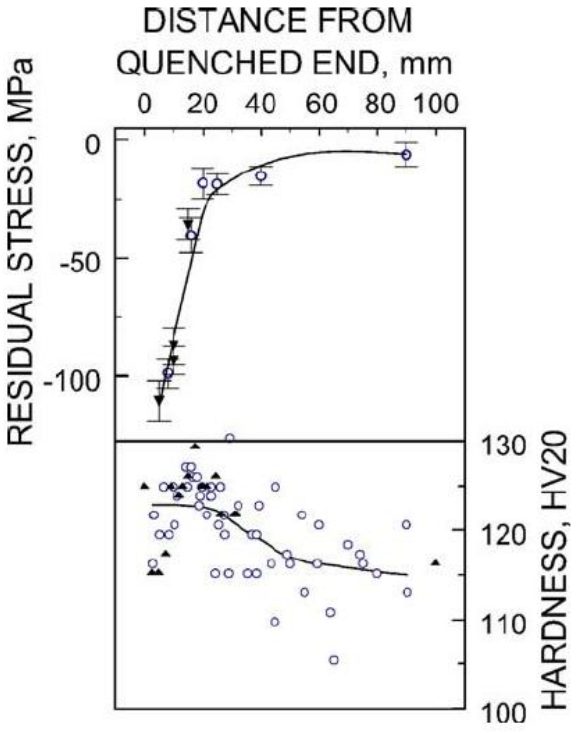

Figure 9 Residual stresses and hardness profile of a 7010 JEQ bar [24]

4. Quench Factor Analysis

Quench Factor Analysis (QFA) is a method predicting properties based on cooling rate and can be applied to the Jominy end quench test. The quench factor is based on the rate of precipitation during cooling which is dependent on supersaturation and diffusion [5]. Quench Factor Analysis as described by [5] is as follows:

The equation for quench factor is represented by

$$\tau = \int(dt/C_t) \quad (1)$$

where τ is the quench factor and C_t is the critical time for a specific percentage of transformation to occur from the TTP curve. The equation for C_t is described by

$$C_t=K_1K_2[\exp(K_3K_4^2/RT(K_4-T)^2)\exp(K_5/RT)] \quad (2)$$

where T is the temperature in Kelvin and R is the universal gas constant. K_1 is a constant equal to $ln(0.995)$ or the fraction untransformed during quenching, K_2 is a constant related to the reciprocal of the number of nucleation sites, K_3 is a constant related to the energy required to form a nucleus, K_4 is a constan related to the solvus temperature, and K_5 is related to the activation energy required for diffusion.

This method uses a C-curve to determine the constants, shown in Figure 10, which is a collection of C_t points and is scarce in the literature for most alloys.

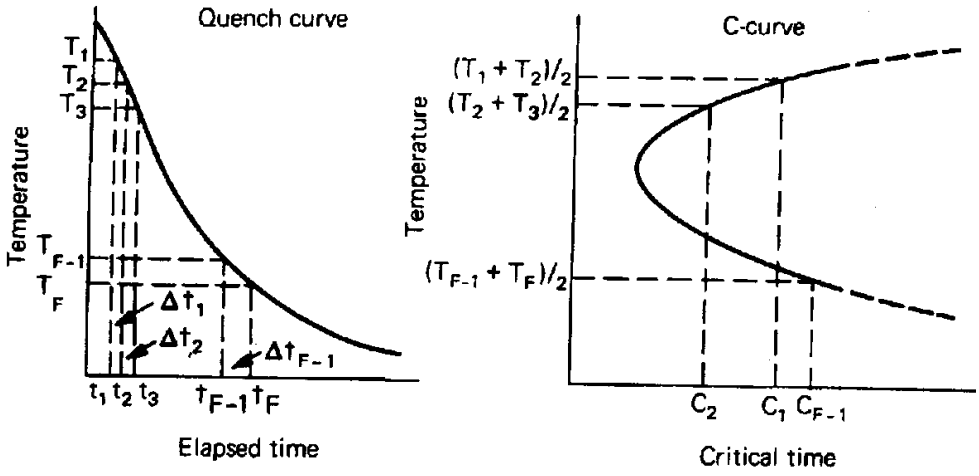

Figure 10 Schematic of how quench factors are calculated [5]

Properties such as hardness, strength, and conductivity can be related to the quench factor by

$$\rho=\rho_{max}e^{k\tau} \tag{3}$$

where ρ_{max} is the maximum attainable property with infinite quench rate.

The cumulative quench factor, *Q*, is the sum of the incremental quench factors which are represented by a series of equations such as

$$\begin{aligned}
\tau_1 &= \Delta t_1/C_1 + \Delta t_2/C_2 + \Delta t_3/C_3 + \ldots + \Delta t_n/C_n \\
\tau_2 &= \Delta t_1/C_1 + \Delta t_2/C_2 + \Delta t_3/C_3 + \ldots + \Delta t_n/C_n \\
\tau_3 &= \Delta t_1/C_1 + \Delta t_2/C_2 + \Delta t_3/C_3 + \ldots + \Delta t_n/C_n \\
\tau_4 &= \Delta t_1/C_1 + \Delta t_2/C_2 + \Delta t_3/C_3 + \ldots + \Delta t_n/C_n
\end{aligned} \tag{4}$$

where Δt is a temperature interval and *C* is the critical time.

5. Effects of Heating Rate

Unlike quench sensitivity, studies on the effects of heating rate are less common in the

literature. An understanding of the effects of heating rate is important in evaluating methods to result in desirable microstructure and properties, as well as cost and time savings during heat treatments. It is important to study different materials as not all results are in agreement for various materials. There have been controversial studies on MnZn and NiZn ferrites [32]. These studies agree that densification is greater with increased heating rate, however a MnZn study contradicts the NiZn studies by concluding that average grain size increases with increasing heating rate [32]. The grain size results from this study are presented as a function of heating rate in Figure 11.

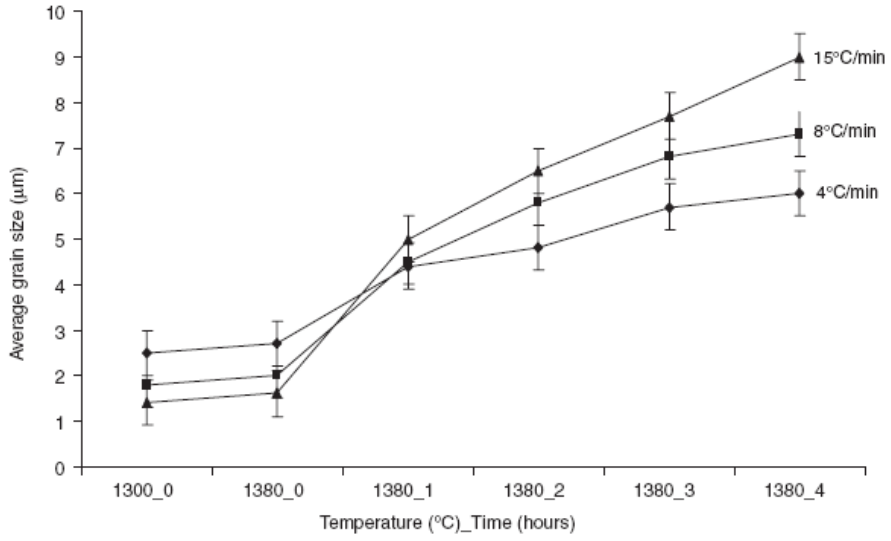

Figure 11 Average grain size of MnZn ferrites with relation to heating rate [32]

There have also been studies on the aluminum alloy LY12 by Peng et al. [33,34]. The results showed that with increased heating rates, more defects occur in the microstructure attributed by local thermal inconsistency (LTI), where some areas were affected more than others by the heating rate. It was also shown that rupture strength is lowered after rapid heating. A study on the effects of heating rate on the continuous cast aluminum

alloy 3105 concludes that elongated recrystallized grains occur after a slow anneal whereas fine equiaxed grains were observed after a rapid anneal and micrographs of this phenomenon are shown in Figures 12 and 13 [35]. The study also showed that a rapid salt bath anneal results in greater tensile strength than that of a slow air furnace anneal.

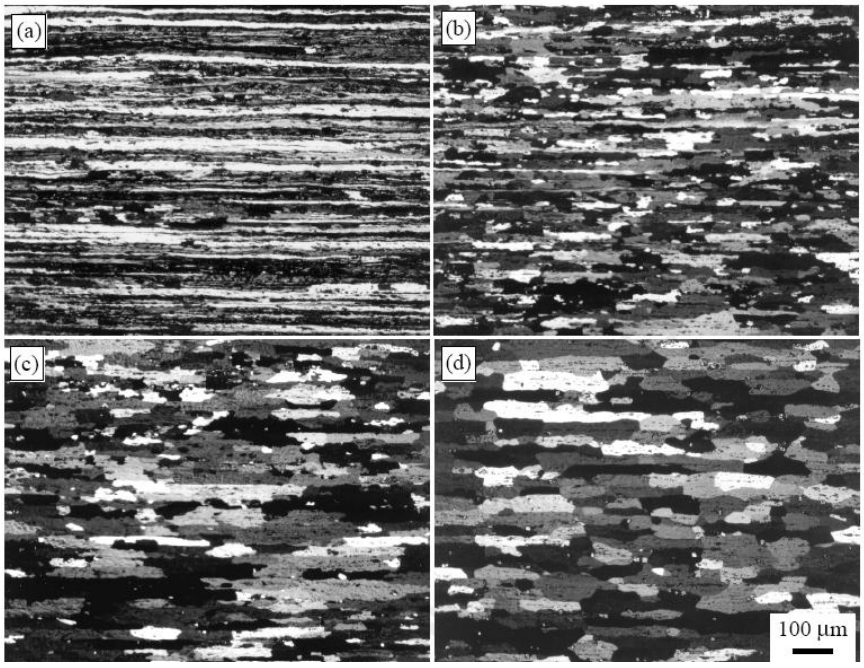

Figure 12 AA3105 after annealing at (a) 371 (b)427 (c) 482 (d) 599^{o}C for 6 h with a heating rate of 11^{o}C/min [35]

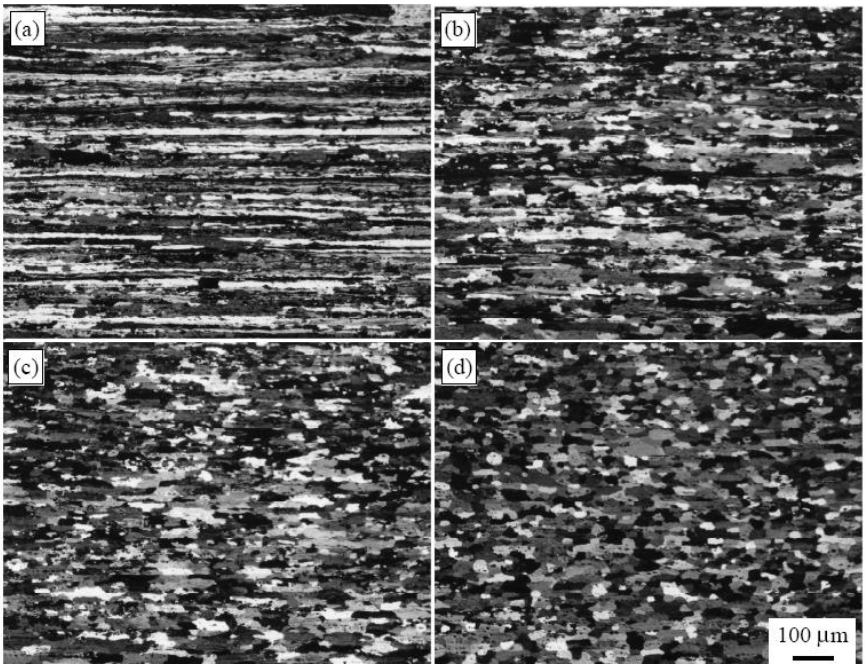

Figure 13 AA3105 after annealing at (a) 427 (b) 454 (c) 482 (d) 599^{o}C for 6 h in a salt bath [35]

A study by Blue et al. [36] at Oak Ridge National Lab (ORNL) shows that rapid infrared preheating of forged products leads to higher fatigue strength than gas infrared which results in a lower heating rate (Fig. 14). Energy savings were also significant and die life was extended. This study is in agreement with [35] that grain size in aluminum alloys is decreased with higher heating rates. The two heating rates used in this study are presented in Figure 15 with their resulting microstructures. A further study at ORNL [37] confirms that fast heating increases grain size in forged products and also increases hardness, yield strength, and fatigue strength.

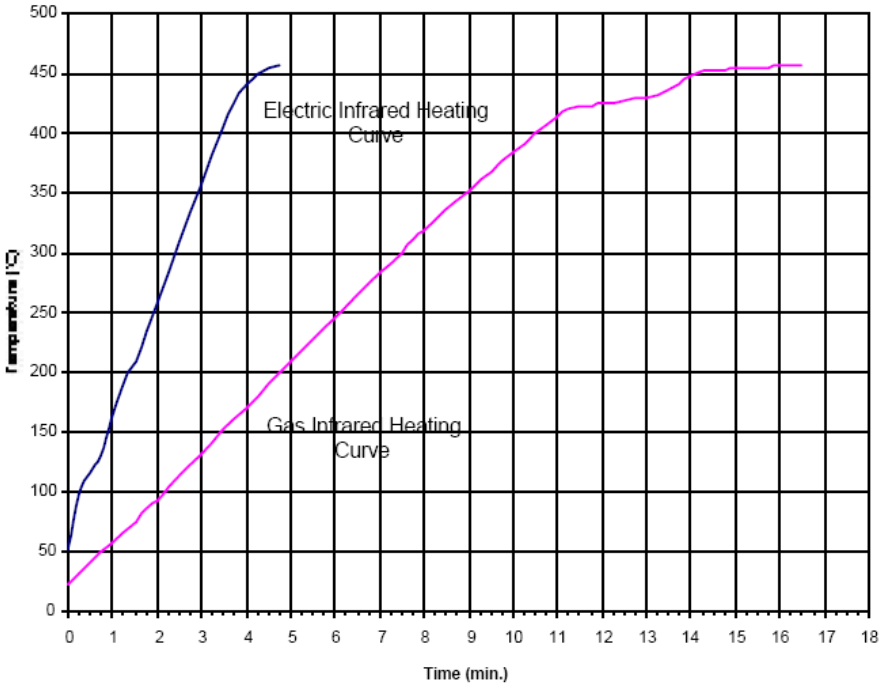

Figure 14 Heating rates of electric infrared versus gas infrared [36]

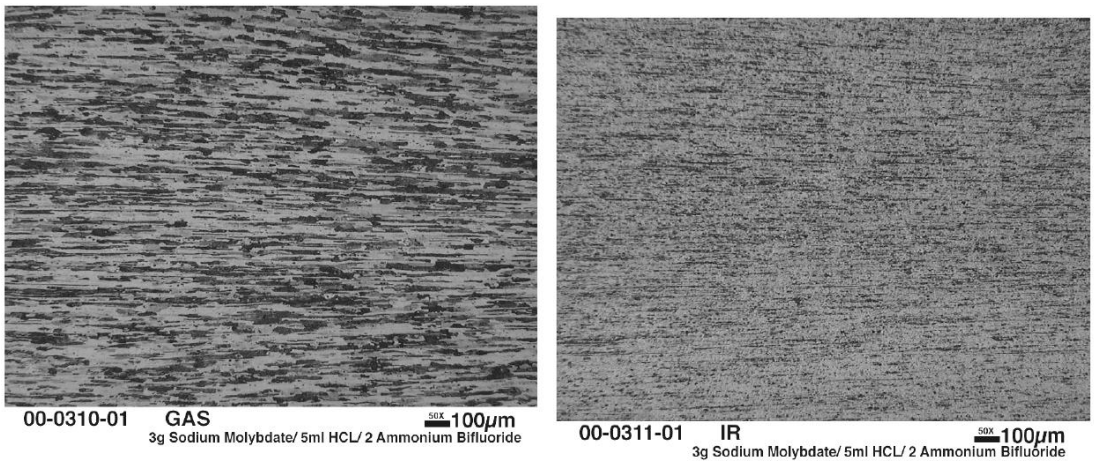

Figure 15 Microstructure after (left) slow heating rate by gas infrared and (right) fast heating by electric infrared [36]

S.S. Sahay and K.B. Joshi [38] found similar results for steel. Figure 16 shows the microstructural changes in grain size with respect to heating rate. They found that increased heating rate leads to smaller, equiaxed grains and that a 67% increase in mean

grain size was observed when cooling rate decreased from 10°C to 1°C [38].

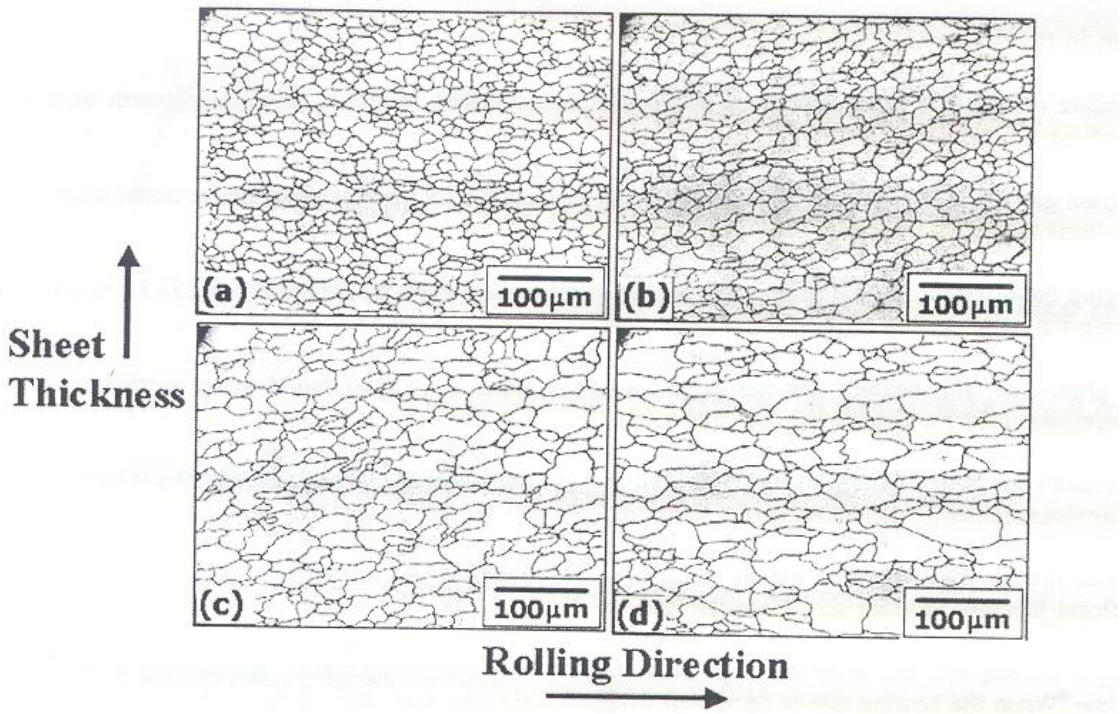

Figure 16 Microstructure of samples annealed at 725°C for 6 h with heating rates of (a) 10°C/min (b) 5°C/min (c) 3°C/min (d) 1°C/min [38]

A study by Deschamps and Bréchet [7] was conducted on a Zr containing 7000 alloy to qualitatively determine the effects of heating rate. Deschamps and Bréchet found that after rapid heating during aging there was a decrease in peak hardening. Another study by Deschamps and Nicolas [39] showed that with rapid heating of Al-Zn-Mg, particles become unstable and dissolve. This results in variations in average grain size since the small particles dissolve much more quickly than larger particles. The effect of heating rate on volume fraction of precipitation is shown in Figure 17. Deschamps et al. [40] found that after rapid heating during aging the initial precipitate radius is larger than after slow heating. Precipitation of η′ is difficult in the rapid heating because of the reversion

of GP zones [40]. Deschamps and Bréchet [41] determined the precipitate radius after fast and slow heating using small angle X-ray scattering which is presented in Figures 18 and 19.

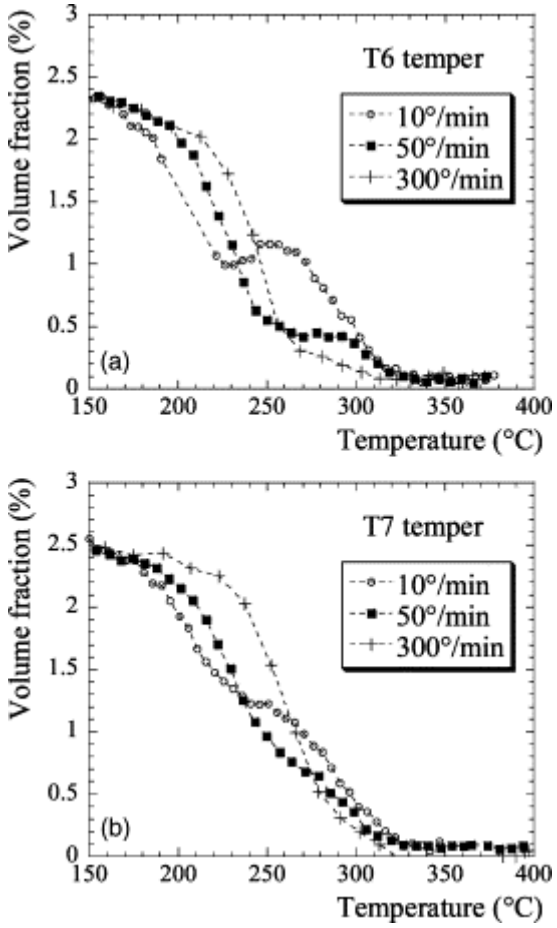

Figure 17 Evolution of volume fraction of (a) T6 and (b) T7 treatments during continuous heating with heating rates of 10^{o}/min, 50^{o}/min, and 300^{o}/min [39]

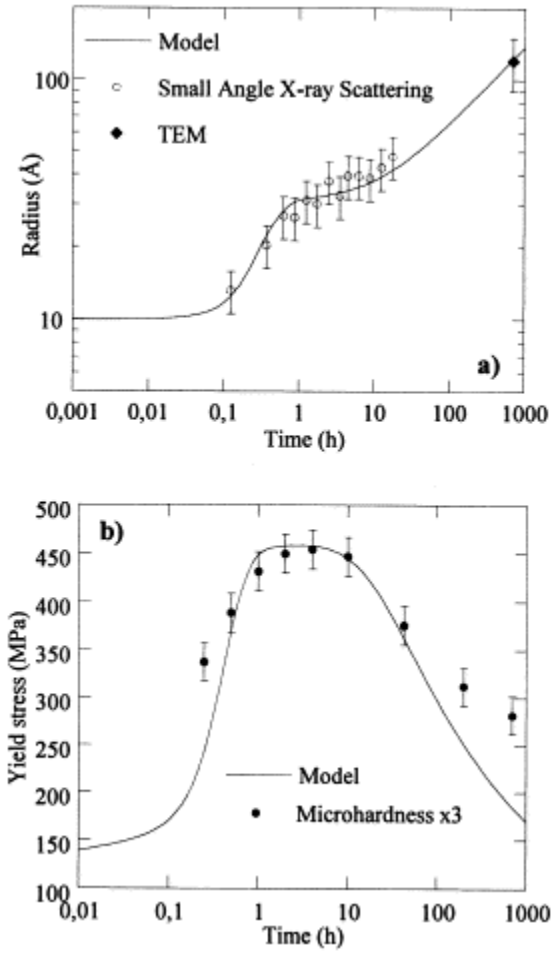

Figure 18 (a) Average radius after fast heating (b) Yield strength after fast heating [41]

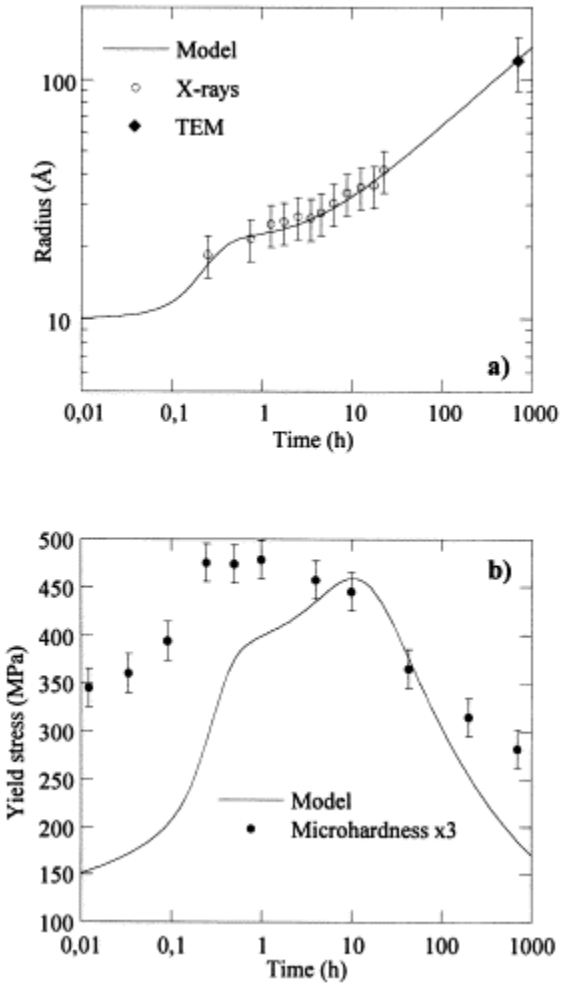

Figure 19 (a) Average radius after slow heating (30^{o}C/hr) (b) Yield strength after slow heating [41]

Bibliography

1. J.E. Hatch (ed.), *Aluminum: Properties and Physical Metallurgy*, 134-199, American Society for Metals, Materials Park, OH (1984)
2. L.F. Mondolfo, *Aluminum Alloys: Structure and Properties*, 842-882, Butterworth & Co Ltd, Boston, MA (1976)
3. S.P. Ringer, B.C. Muddle, I.T. Polmear, *Metall. Trans.*, 26A, 1659, (1995)
4. L Katgerman and D. Eskin, *Hardening, Annealing, and Aging*, Handbook of Aluminum , Vol. 1, 881-970, Marcel-Dekkar, Inc., New York, NY (2003)
5. R. Howard, N. Bogh and D.S. Mackenzie, *Heat Treating Processes and Equipment*, Handbook of Aluminum , Vol. 1, 881-970, Marcel-Dekkar, Inc., New York, NY (2003)
6. J.W. Bray, *ASM Handbook Vol. 2*, 29-122, ASM International, Materials Park, OH (1990)
7. A. Deschamps, Y. Bréchet, Influence of quench and heating rates on the ageing response of an Al-Zn-Mg-(Zr) alloy, *Materials Science and Engineering* A251 (1998) 200-207
8. D. Thevenet, M. Mliha-Touati, A. Zeghloul, The effect of precipitation on the Portevin-Le Chatelier effect in an Al-Zn-Mg-Cu alloy, *Materials Science and Engineering* A266 (1999) 175-182
9. N.Q. Chinh, J. Lendvai, D.H. Ping and K. Hono, The effect of Cu on mechanical and precipitation properties of Al-Zn-Mg alloys, *Journal of Alloys and Compounds* 378 (2004) 52-60
10. B.C. Wei, C.Q. Chen, Z. Huang, Y.G. Zhang, Aging behavior of Li containing Al-Zn-Mg-Cu alloys, *Materials Science and Engineering* A280 (2000) 161-167
11. R. Ferragut, A. Somoza, A. Tolley, Microstructural evolution of 7012 alloy during the early stages of artificial ageing, *Acta Materialia* Vol 47 No 17 (1999) 4355-4364
12. B.M. Gamble, A.A. Csontos, E.A Starke Jr., A quench sensitivity study on the novel Al-Li-Cu-X alloy AF/C 458, *Journal of Light Metals* 2 (2002) 65-75
13. Liu SD et al. Influence of aging on quench sensitivity effect of 7055 aluminum

alloy. *Mater Charact* (2006), doi:10.1016/j.matchar.2006.10.1019

14. J.C. Werenskiold, A. Deschamps, Y. Bréchet, Characterization and modeling of precipitation kinetics in an Al-Zn-Mg alloy. *Materials Science and Engineering* A293 (2000) 267-274
15. Z. Li et al. Investigation of microstructural evolution and mechanical properties during two-step ageing treatment at 115 and 160^{o}C in an Al-Zn-Mg-Cu alloy pre-stretched thick plate, *Mater Charact* (2007), doi:10.1016/j.matchar.2007.01.006
16. M.J. Starink and X.M. Li, A Model for the Electrical Conductivity of Peak-Aged and Overaged Al-Zn-Mg-Cu Alloys, *Metallurgical and Materials Transactions A* 34A (2003) 899-910
17. M.J. Starink, S.C.Wang, A model for the yield strength of overaged Al-Zn-Mg-Cu alloys, *Acta Materialia* 51 (2003) 5131-5150
18. X. Fan, D. Jiang, Q. Meng, L. Zhong, The microstructural evolution of an Al-Zn-Mg-Cu alloy during homogenization, *Materials Letters* 60 (2006) 1475-1479
19. C. Wolverton, Crystal structure and stability of complex precipitate phases in Al-Cu-Mg-(Si) and Al-Zn-Mg alloys, *Acta Materialia* 49 (2001) 3129-3142
20. T. Engdahl, V. Hansen, P.J. Warren, K. Stiller, Investigation of fine scale precipitates in Al-Zn-Mg alloys after various heat treatments, *Materials Science and Engineering* A327 (2002) 59-64
21. L.L. Rokhlin, T.V. Dobatkina, N.R. Bochvar, E.V. Lysova, Investigation of phase equilibria in alloys of the Al-Zn-Mg-Cu-Zr-Sc system, *Journal of Alloys and Compounds* 367 (2004) 10-16
22. P. Archambault, D. Godard, High temperature precipitation kinetics and TTT curve of a 7xxx alloy by in-situ electrical resistivity measurements and differential calorimetry. *Scripta Materialia* 42 (2000) 675-680
23. G.E. Totten, G.M. Webster and C.E. Bates, *Quenching*, Handbook of Aluminum , Vol. 1, 881-970, Marcel-Dekkar, Inc., New York, NY (2003)
24. D.A. Tanner, J.S. Robinson, Effect of precipitation during quenching on the mechanical properties of the aluminium alloy 7010 in the W-temper, *Journal of Materials Processing Technology* 153-154 (2004) 998-1004
25. S.T. Lim, S.J. Yun, S.W. Nam, Improved quench sensitivity in modified aluminum

alloy 7175 for thick forging applications, *Materials Science and Engineering* A371 (2004) 82-90

26. A. Deschamps, Y. Bréchet, Nature and distribution of quench-induced precipitation in an Al-Zn-Mg-Cu alloy, *Scripta Materialia* Vol 39 No 11 (1998) 1517-1522
27. ASTM A255, *Standard Test Method for Determining the Hardenability of Steel*, ASTM, (2007)
28. D.S. Mackenzie, *Quench Rate and Aging Effects in Al-Zn-Mg-Cu Aluminum Alloys*, PhD Dissertation, University of Missouri-Rolla (2000)
29. D.S. Mackenzie, Private Communication, *Quench Sensitivity of 7136 Aluminum*, Houghton International Inc., Valley Forge, PA, (2007)
30. S. Ma, *A Methodology to Predict the Effects of Quench Rates on Mechanical Properties of Cast Aluminum Alloys*, PhD Dissertation, Worcester Polytechnic Institute, Worcester, MA (2006)
31. S. Ma, M. Maniruzzaman, D.S. MacKenzie and R.D. Sisson, Jr. *A Methodology to Predict the Effects of Quench Rates on Mechanical Properties of Cast Aluminum Alloys*, accepted for publication in Met. Trans B, (2007)
32. V.T. Zaspalis, S. Sklari, M. Kolenbrander, The effect of heating rate on the microstructure and properties of high magnetic permeability MnZn-ferrites, *Journal of Magnetism and Magnetic Materials* 310 (2007) 28-36
33. X. Peng, J. Fan, Y. Yang, Y. Chen, Y. Yin, Investigations to the effect of heating-rate on the thermomechanical properties of aluminum alloy LY12, *International Journal of Solids and Structures* 40 (2003) 7385-7397
34. X. Peng, X. Zhang, J. Fan, B. Chen, Effect of heating-rate on the thermomechanical behavior of aluminum alloy LY12 and a phenomenological description, *International Journal of Solids and Structures* 43 (2006) 3527-3541
35. W.C. Liu, A. Li, C.-S. Man, Effect of heating rate on the microstructure and texture of continuous cast AA 3105 aluminum alloy, *Materials Science & Engineering A* (2007), doi:10.1016/j.msea.2007.05.107
36. C.A. Blue, V.K. Sikka, E.K. Ohriner, P.G. Engleman, G.F. Mochnal, A. Underys, W-T. Wu, M.C. Maguire and R. Mayer, *Infrared Heating of Forging Billets and Dies*, UT-Batelle, LLC

37. P. Kadolkar, H. Lu, C. Blue, T. Ando, R. Mayer, Application of rapid infrared heating to aluminum forgings, *25th Forging Industry Technical Conference*, Detroit, MI (2004)
38. S.S. Sahay, K.B. Joshi, Heating rate effects during non-isothermal annealing of AIK steel, *Journal of Materials Engineering and Performance* 12 (2003) 157-164
39. M. Nicolas, A. Deschamps, Characterisation and modeling of precipitate evolution in an Al-Zn-Mg alloy during non-isothermal heat treatments, *Acta Materialia* 51 (2003) 6077-6094
40. A. Deschamps, F. Livet, Y. Bréchet, Influence of predeformation on ageing in an Al-Zn-Mg alloy—I. Microstructure evolution and mechanical properties, *Acta Materialia* Vol. 47 No. 1 (1999) 281-292
41. A. Deschamps, Y. Bréchet, Influence of predeformation and ageing of an Al-Zn-Mg alloy—II. Modeling of precipitation kinetics and yield stress, *Acta Materialia* Vol. 47 No. 1 (1999) 293-305

Chapter III

Aging Behavior of AA7136

by C. Nowill, M. Maniruzzaman, R.D. Sisson, Jr., and D.S. Mackenzie

Materials Science and Engineering, Mechanical Engineering Department, WPI,

Worcester, MA 01609

Abstract

The 7000 series of aluminum alloys are primarily used in the aerospace industry as structural components and are strengthened by age-hardening. The AA7136 wrought aluminum alloy is an Al-Zn-Mg-Cu-Zr alloy. Limited data for the aging kinetics of this particular alloy is available in the literature. A series of Jominy end-quench tests were performed to investigate the effect of cooling rate on the aging performance of the alloy. The process variables used in this study is aging time and temperature. Natural aging experiments were also conducted to verify the hardenability of the alloy at room temperature. In this study the Jominy end quench data is used to determine quench sensitivity of the alloy.

Introduction

The 2000, 6000, and 7000 series of aluminum alloys are precipitation or age-hardenable. During age-hardening precipitates form in a supersaturated solid solution and strength increases as the number and size of precipitates increase until a maximum value is reached and the material becomes overaged and coarsening begins, reducing the strength of the alloy [1]. The 7000 series is comprsed of Al-Zn-Mg-Cu alloys where zinc is the strengthening component [2]. These alloys are primarily used in the aerospace and automotive industries because of their high strength and heat treatability. In aluminum alloys with greater than 3% Zn and a Zn to Mg ratio greater than 2, the hardening phase

is $MgZn_2$ (η) [2]. Precipitates in these alloys start as GP zones which become η′ coherent platelets and transform to η over time [3].

Jominy end quench (JEQ) experiments allow for the determination of a material's sensitivity to cooling rate [4]. Maximum age-hardening occurs with a rapid quench [1]. The experiment consists of a cylindrical bar which is quenched at one end, resulting in a distribution of cooling rates throughout the bar. Mechanical properties can then be related to quench rate. Jominy end quench was first used to determine the hardenability of steels and many studies have shown that this test can be applied to nonferrous alloys as well [5].

In this study the Jominy end quench experiments are used to determine the effects of cooling rate on the hardness of AA7136. A number of other experiments were also conducted to determine the effect of aging temperature and precipitate formation.

Experimental Procedure

The composition of the AA7136 is presented in Table 1. This composition was analyzed by JMatPro [6], a materials property modeling software based on CALPHAD method [7] which can predict phase equilibria in multi-component alloys. Round bars, 2.54 cm diameter, 10.2 cm long, were prepared from the received material to serve as Jominy end quench bars according to ASTM A255 [4].

Table 1: Composition by Spectro Analysis

Si	Fe	Cu	Mg	Zn	Zr	Al
0.029	0.073	2.152	1.936	8.542	0.127	87.06

For the heat treatment of JEQ bars, the industrial T6 heat treatment used for many 7000 alloys was prescribed (aged at 121℃ for 24 hours) [8]. JEQ bars were aged at 250℃ for various times. The test matrix is presented in Table 2. Thermocouples were placed at 1.27cm, 5.08cm, and 7.62cm from the quench end of the bars in order to record cooling rate using LabVIEW 6.1. Solutionizing was done in a tube furnace and quenching took place in a JEQ apparatus built according to the ASTM standard (Fig.1). Samples were transferred from the furnace to the quenching apparatus in less than five seconds. Once the bars cooled to 6-8℃, the temperature of the quenching water, they were placed in a conventional freezer for holding. The bars were aged in a small box furnace according to the test matrix and quenched in ice water. Again, the bars were placed in a freezer for holding.

Table 2: Test Matrix for JEQ bar heat treatment

Sample No.	Solution Treatment; Aging Treatment
1	475°C, 5hr; 121°C, 24hr
2	475°C, 5hr; 250°C, 2hr
3	475°C, 5hr; 250°C, 10hr
4	475°C, 5hr; 250°C, 24hr

Figure 1: Jominy End Quench (JEQ) apparatus

Hardness profiles were obtained using a Rockwell B scale on a Wilson digital Rockwell hardness tester, which was calibrated against a standard. Four sides of each bar, about 90° apart, were milled to 0.381 mm from the surface, according to the ASTM standard. Hardness testing was conducted on each bar, starting from the quenched end at intervals as specified by the standard.

Cross sections of the heat treated JEQ bars were mounted in Bakelite and polished using SiC papers, 1 micron alumina, and finished with Buehler Mastermet silica polishing

suspension. Samples were etched using Keller's Reagent. Optical and SEM microscopy was conducted.

To determine the effects of aging temperature on AA7136, several samples were cut into pieces about 1cm x 1cm x 2.5cm. These were heat treated and aged according to the test matrix shown in Table 3. After solution treatments the samples were quenched in ice water, except for one, which was air cooled. The artificially aged samples were quenched in ice water and held in a freezer, while the naturally aged samples were placed at room temperature. Hardness was conducted similarly to the JEQ bars on the Rockwell B scale. TEM studies on these samples are underway in order to study the precipitate formation during aging of this alloy.

Table 3: Test Matrix 2

Sample No.	Solution Treatment; Aging Treatment
1	as-received
2	475°C, 5hr; air cool
3	475°C, 5hr; room temperature age
4	475°C, 5hr; 121°C, 4hr
5	475°C, 5hr; 121°C, 10hr
6	475°C, 5hr; 121°C, 24hr
7	475°C, 5hr; 121°C, 100hr
8	475°C, 5hr; 180°C, 10hr
9	475°C, 5hr; 250°C, 10hr

In addition, a bar of AA7075 underwent the same T6 JEQ test for comparison purposes, since this alloy has been extensively studied.

Results and Discussion

Spectro and JMatPro Data

The composition of the as-received AA7136 presented in Table 1 and AA7075 was analyzed by JMatPro and the calculated TTT diagram is shown in Figure 2. The diagrams show the start of transformation (0.5% amount of phase formed) of various phases from the supersaturated Al phase. At temperatures below 180^{o}C, the GP zone formation is favored and the kinetics are very rapid. The precipitation hardening mechanisms in 7000

alloys are based on three phases or the metastable forms of these phases; (1) η-$MgZn_2$, (2) T–AlCuMgZn and (3) S-Al_2CuMg. The results of the AA7136 TTT diagram were used in determining a test matrix for aging heat treatment.

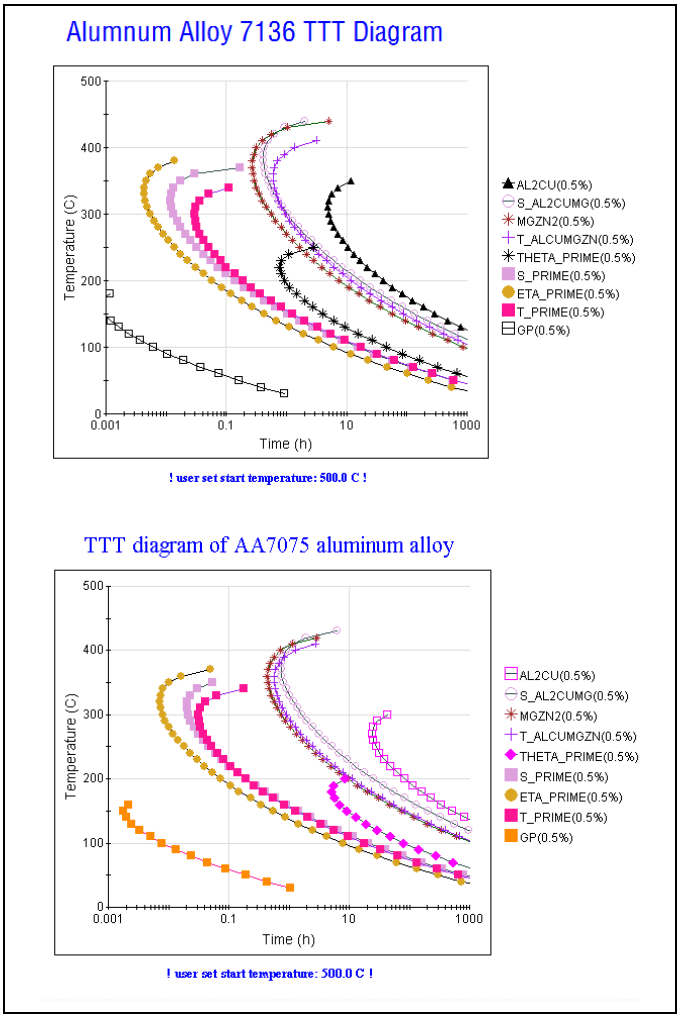

Figure 2: Calculated TTT Diagram for (top) AA7136 and (bottom) AA7075 using JMatPro [6]

Figure 3 shows the metastable phases that may form during the aging heat treatment of AA7136 alloy. As shown in the figure, η' phase will form in substantial amounts in the temperature range of 100 – 250°C, that of used for aging in this study.

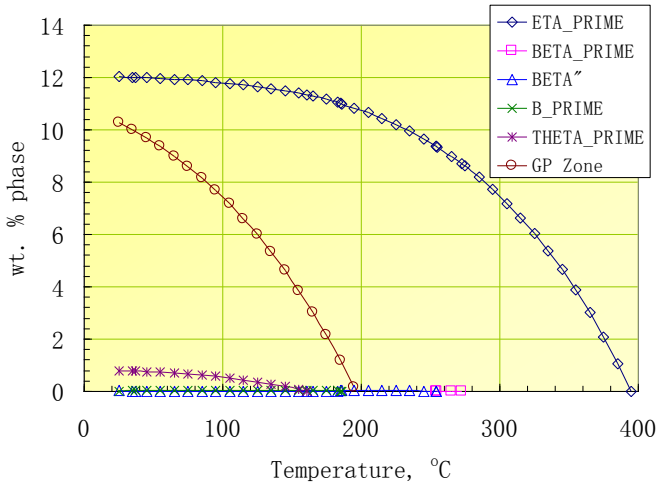

Figure 3: Calculated phase % vs. temperature plot for metastable phases in AA7136 alloy. GP calculation assumes other phases are not formed

Cooling Data

The cooling data for AA7136 correlated with the data for AA7075 as well as the cooling data for A356, studied by S. Ma [9] (Fig. 4). In all alloys the cooling rates were close to the same after about 25 seconds. AA7136 experienced a maximum cooling rate at 12.7 mm from the quenched end of about 30°C/s, while 50.8 mm from the quenched end reached a maximum of about 22°C/s. AA7075 had maximum cooling rates of about 45°C/s and 26°C/s at 12.7 mm and 50.8 mm, respectively.

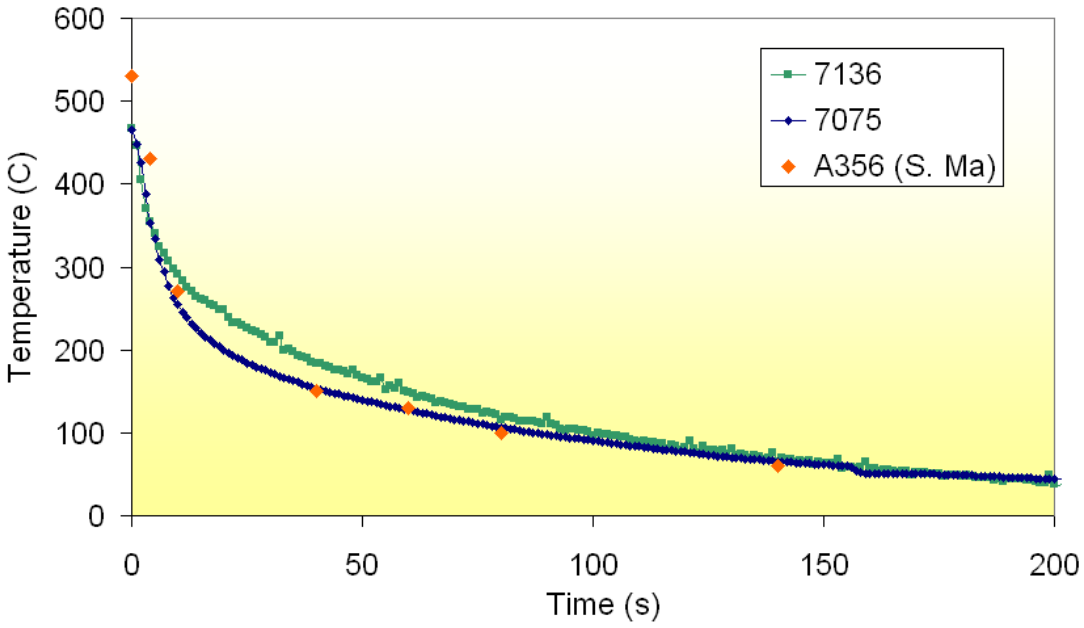

Figure 4 Time-temperature data at 1.3 cm from quenched end during JEQ for AA7136 and AA7075 compared to A356 by [9]

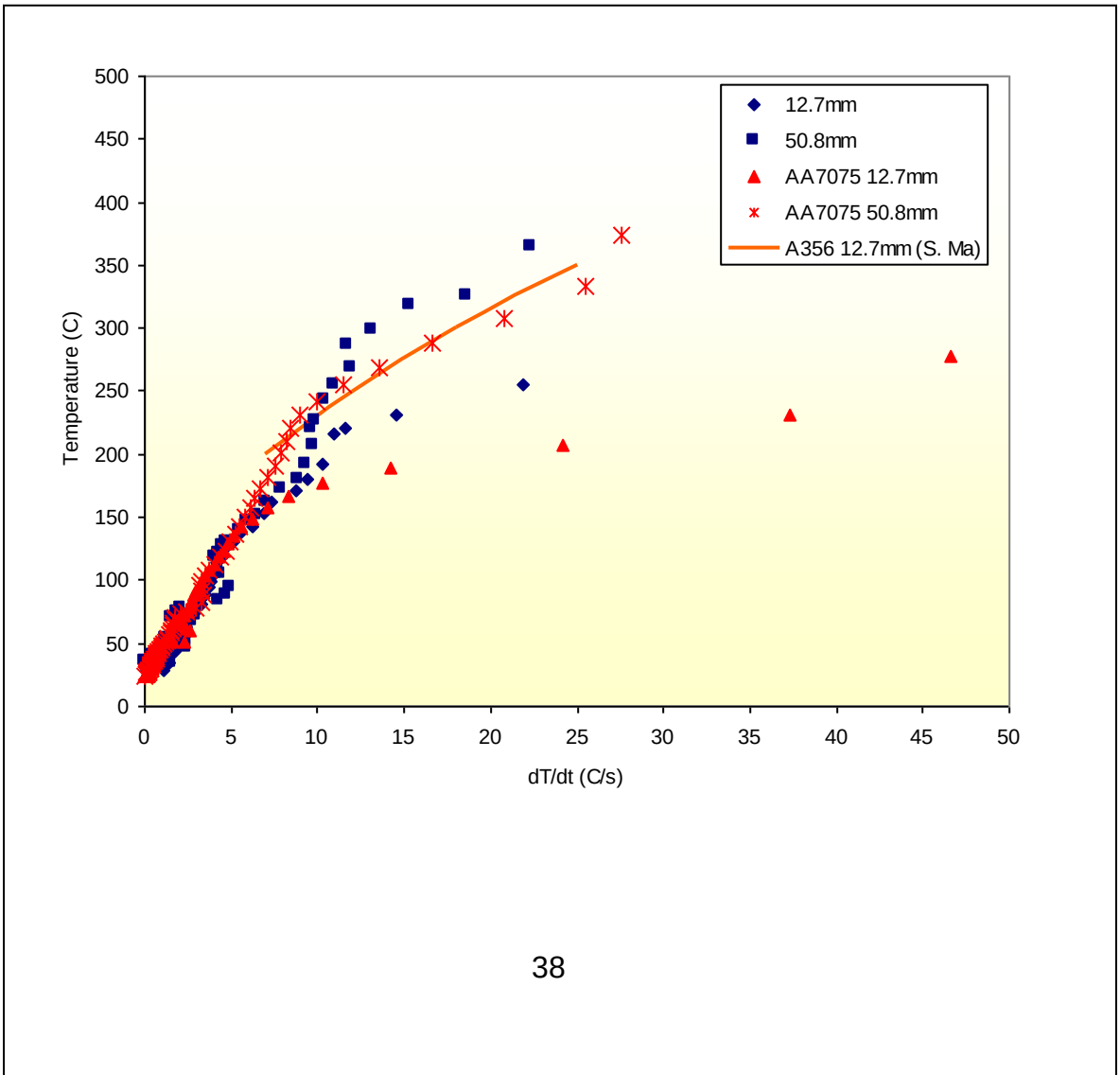

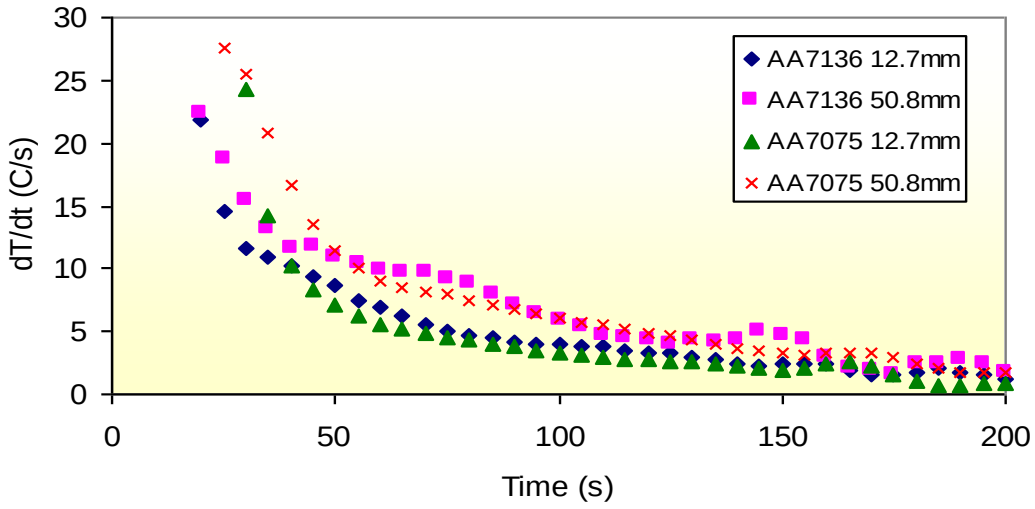

Figure 5 Time-temperature data at 1.3 cm from quenched end during JEQ for AA7136 and AA7075 compared to A356 by [9]

Hardness Profiles

The hardness profile for AA7136 alloy that was solutionized for 5 hours at 475^{o}C is presented in Figure 6. As seen in the figure, the bars aged at 250°C were overaged, showing Rockwell B values of less than 35, much lower than the JEQ bar aged at 121°C. Since the hardness values only vary by a maximum of 7.5 HRB, the alloy is somewhat quench rate insensitive. The results of the AA7075 JEQ specimen are presented with the results of D.S. Mackenzie [10] in Figure 7. The data from [10] was converted from Vickers to HRB and the data sufficiently matches the hardness profile from this study. Figure 8 is a comparison of AA7136 and similar commercial alloys, AA7075 and

AA7050 [11]. The figure shows that AA7136 is considerably less quench sensitive than aluminum alloys 7075 and 7050.

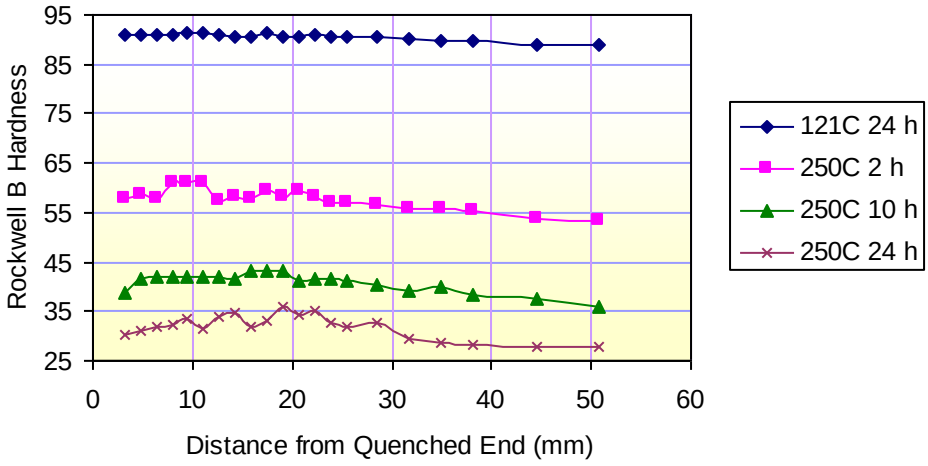

Figure 6: Hardness Profiles on Jominy End Quench (JEQ) bars

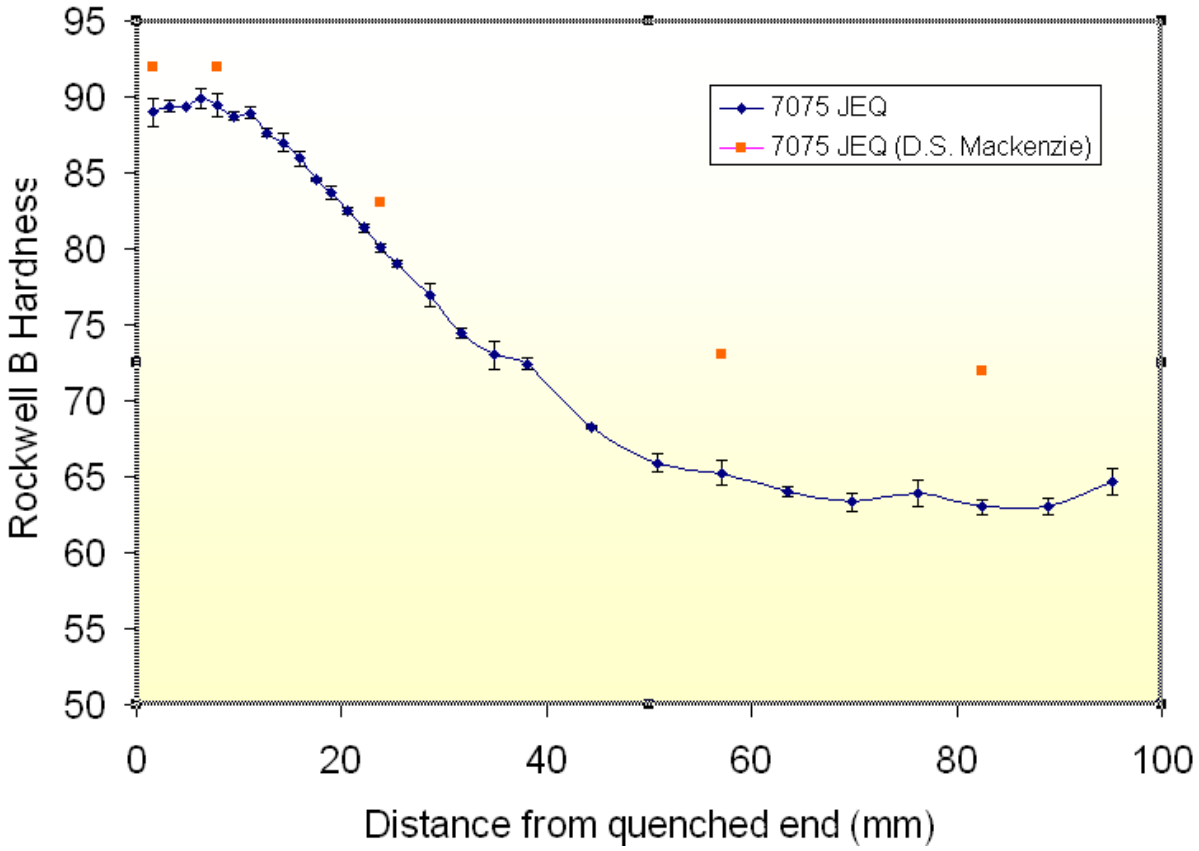

Figure 7: Hardness Profile of AA7075 compared to the results by D.S. Mackenzie [10]

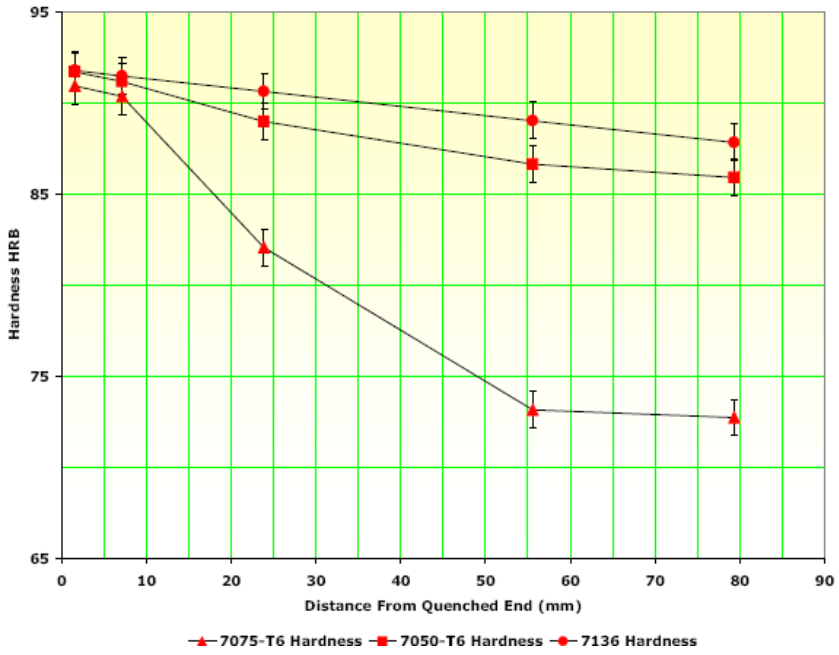

Figure 8: Hardness profiles of selected 7000 alloys [11]

Figure 9 presents average HRB after various aging temperatures. The highest average hardness values were heat treated at 121°C, 180°C, and room temperature. The sample heat treated at 250°C is clearly overaged with an average value about 40 HRB.

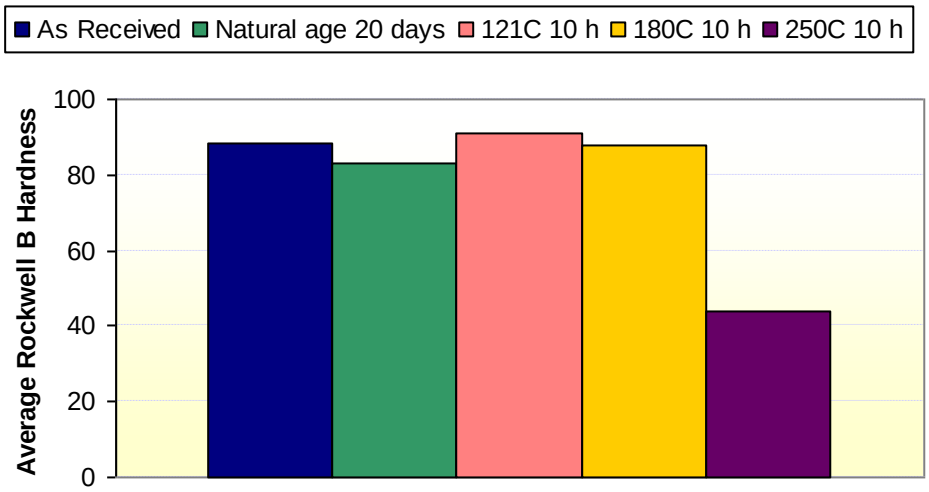

Figure 9: Average Rockwell B values for various samples

Figure 10 presents the aging kinetics of AA7136 for natural aging as well as artificial aging at 121^{o}C. Five minutes after quenching from solution treatment resulted in average hardness of 44 HRB, which increased to 60 after 1 day, 69 after 4 days and 84 after 20 days in case of natural aging. On the other hand peak hardness of 92 HRB is reached after 24 hours at 121°C.

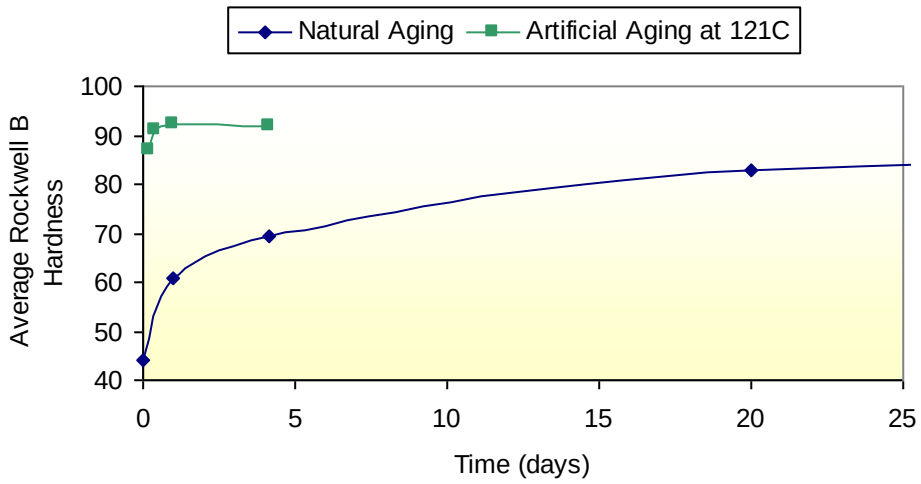

Figure 10: Aging Curves of AA7136

Microstructure

The microstructure of as-received AA7136 is shown in Figure 11. As seen in the photomicrograph, the microstructure consists of equiaxed grains of α-Al with various intermetallic and precipitate phases at the grain boundaries. Figure 12 presents the scanning electron microscopy (SEM) image of age hardened AA7136 alloy. Energy Dispersive X-ray (EDX) analysis, as shown in Figure 13, was performed on the

precipitates along grain boundaries. EDX revealed that the precipitates in age hardened AA7136 after the T6 temper were Al-Cu-Mg-Zn.

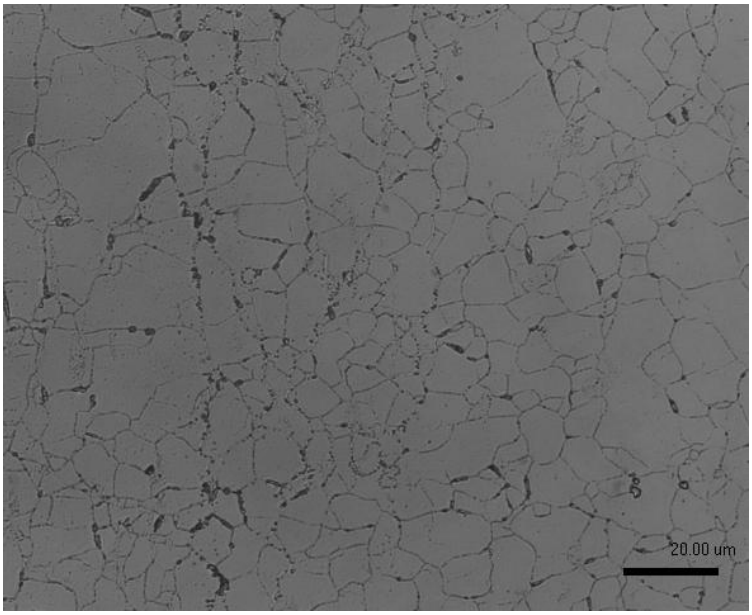

Figure 1: Photomicrograph of the as-received AA7136 alloy, etched with Keller's Reagent

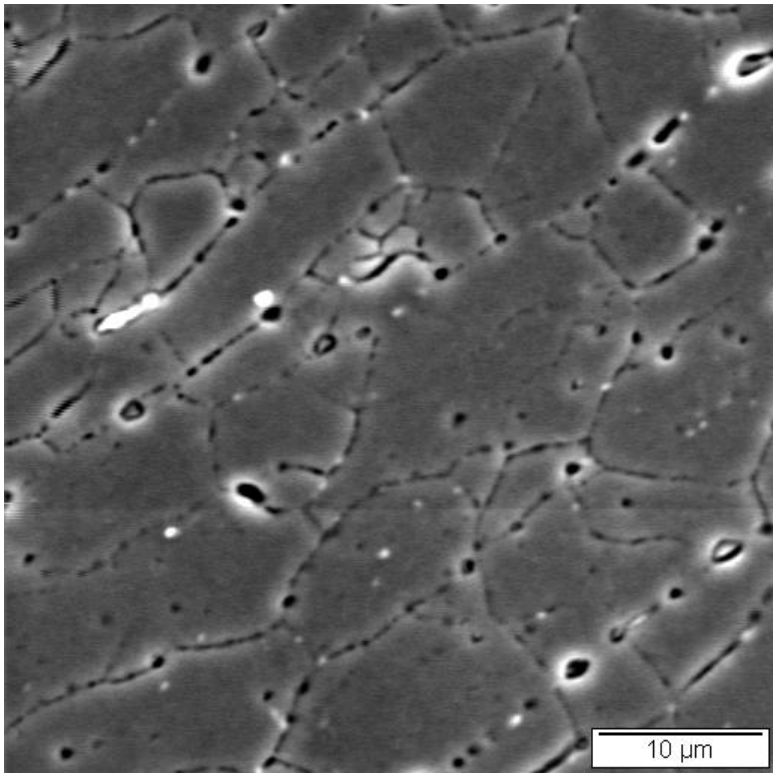

Figure 12: SEM image of aged hardened AA7136 alloy etched with Keller's Reagent

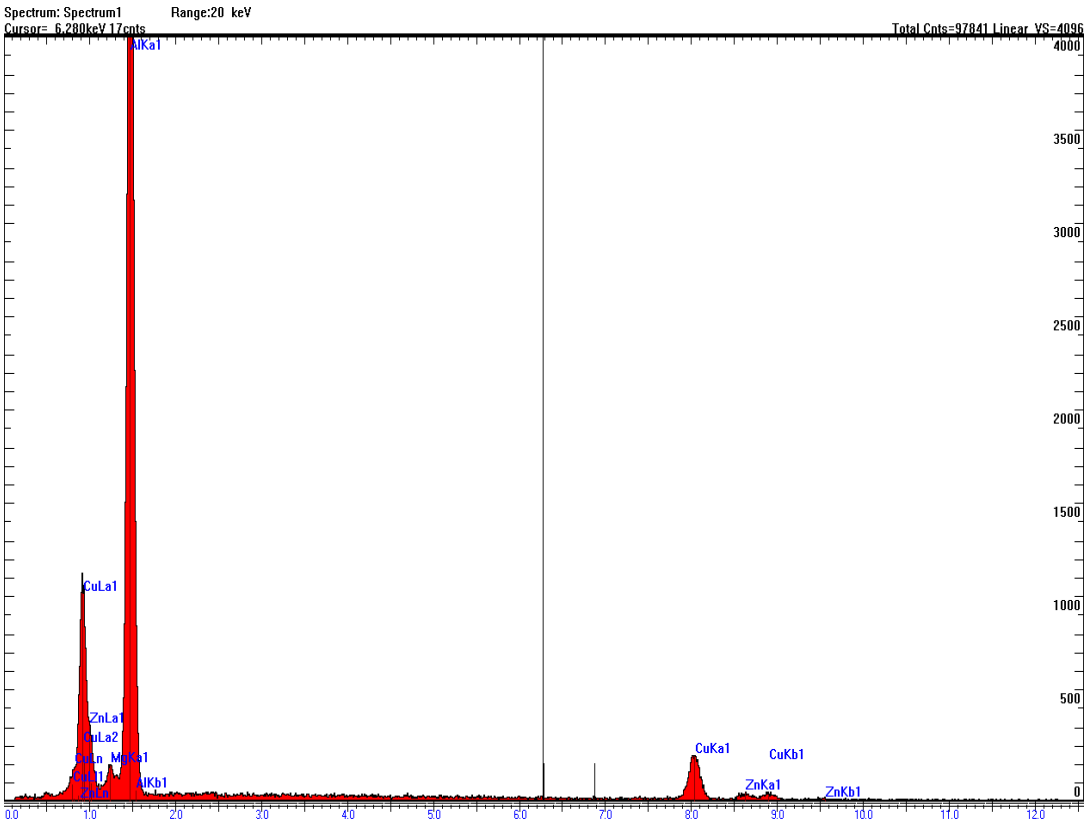

Figure 13: EDX at 14000X on a grain

Future Work

Transmission Electron Microscopy (TEM) analysis, which is currently underway, will determine the identity of the precipitates that form and help clarify the aging kinetics of AA7136. More aging experiments should be conducted to provide information on the performance of this alloy under various conditions. Quench factor analysis based on the Jominy end-quench test data is currently underway, that will allow for the determination of a C-curve, thus allowing property prediction in this alloy [9,10]. Further research will

allow for a better understanding of the properties and phase transformations in this material, allowing possible applications for AA7136 to be identified.

Summary

The Jominy end quench tests revealed that the AA7136 alloy is not quench rate sensitive. Experiments show that after 20 days the average HRB increases from about 44 after solutionizing to about 83 at room temperature, proving that the alloy naturally ages. The experiments conducted in this study also show that peak hardness occurs after artificially aging at 121℃ for 24 hours.

References

1. J.E. Hatch (ed.), *Aluminum: Properties and Physical Metallurgy*, 134-199, American Society for Metals, Materials Park, OH (1984)
2. L.F. Mondolfo, *Aluminum Alloys: Structure and Properties*, 842-882, Butterworth & Co Ltd, Boston, MA (1976)
3. S.P. Ringer, B.C. Muddle, I.T. Polmear, *Metall. Trans.*, 26A, 1659, (1995)
4. ASTM A255, *Standard Test Method for Determining the Hardenability of Steel*, ASTM, (2007)
5. D.S. Mackenzie, *Quench Rate and Aging Effects in Al-Zn-Mg-Cu Aluminum Alloys*, PhD Dissertation, University of Missouri-Rolla (2000)
6. JMatPro, *JMatPro User Manual*, Thermotech Ltd/ Sente Software Ltd., Surrey

Technology Centre, 40 Occam Road, GU2 7YG, UNITED KINGDOM

7. N. Saunders and A.P. Miodownik, *CALPHAD – A Comprehensive Guide*, Elsevier Science, Oxford (1998)
8. J.W. Bray, *ASM Handbook Vol.2*, 29-122, ASM International, Materials Park, OH (1990)
9. S. Ma, *A Methodology to Predict the Effects of Quench Rates on Mechanical Properties of Cast Aluminum Alloys*, PhD Dissertation, Worcester Polytechnic Institute, Worcester, MA (2006)
10. S. Ma, M. Maniruzzaman, D.S. MacKenzie and R.D. Sisson, Jr. *A Methodology to Predict the Effects of Quench Rates on Mechanical Properties of Cast Aluminum Alloys*, accepted for publication in Met. Trans B, (2007)
11. D.S. Mackenzie, Private Communication, *Quench Sensitivity of 7136 Aluminum*, Houghton International Inc., Valley Forge, PA, (2007)

Study of the Effects of Heating Rate on 7000 Series Aluminum Alloys

by C. Nowill, M. Maniruzzaman, S. Shivkumar, and R.D. Sisson, Jr.

Materials Science and Engineering, Mechanical Engineering Department, WPI,

Worcester, MA 01609

Abstract

The quench sensitivity of various steels and aluminum alloys has been studied with the use of the Jominy end quench test (ASTM A255). Some studies have shown that heating rates also have an effect on mechanical properties, but data is scarce in the literature. A methodology has been developed in order to study the effects of heating rates. The apparatus designed is for a type of "reverse" Jominy test which makes use of a standard Jominy bar and results in one dimensional heating throughout the specimen, and therefore, a distribution of heating rates. Two 7000 series alloys, AA7075 and AA7136, were heated using this method to study the effects of heating rate on both solution and aging heat treatments. The effects of a rapid heat up by immersion in a salt bath were also studied versus the effects of a slow air furnace heat up. This study provides a better understanding of the effects of heating rate on 7000 series aluminum alloys.

Introduction

Unlike quench sensitivity, studies on the effects of heating rate are less common in the literature. An understanding of the effects of heating rate is important in evaluating methods to result in desirable microstructure and properties, as well as cost and time savings during heat treatments. It is important to study different materials as not all results are in agreement for various materials. There have been controversial studies on MnZn and NiZn ferrites [1]. These studies agree that densification is greater with increased heating rate, however a MnZn study contradicts the NiZn studies by concluding that average grain size increases with increasing heating rate [1].

There have also been studies on LY12, an Al-Cu-Mg-Mn alloy, by Peng et al. [2,3]. The results showed that with increased heating rates, more defects occur in the microstructure attributed by local thermal inconsistency (LTI), a phenomenon where some areas were affected more than others by the heating rate. It was also shown that rupture strength is lowered after rapid heating. A study on the effects of heating rate on the continuous cast aluminum alloy 3105 concludes that elongated recrystallized grains occur after a slow anneal whereas fine equiaxed grains were observed after a rapid anneal [4]. The study also showed that a rapid salt bath anneal results in greater tensile strength than that of a slow air furnace anneal.

A study by Blue et al. [5] at Oak Ridge National Lab (ORNL) shows that rapid infrared preheating of forged products leads to higher fatigue strength than gas infrared which results in a lower heating rate. Energy savings were also significant and die life was extended. This study is in agreement with [4] that grain size in aluminum alloys is decreased with higher heating rates. A further study at ORNL confirms that fast heating increases grain size in forged products and also increases hardness, yield strength, and fatigue strength [6].

S.S. Sahay and K.B. Joshi [7] found similar results for steel. They found that increased heating rate leads to smaller, equiaxed grains and that a 67% increase in mean grain size was observed when cooling rate decreased from 10^{o}C to 1^{o}C [7].

This study was performed to examine the effects of heating rate on 7000 series, Al-Zn-Mg-Cu, alloys where either zirconium or chromium are added as dispersoids. A study by Deschamps and Bréchet [8] was conducted on a Zr containing 7000 alloy to qualitatively determine the effects of heating rate. Deschamps and Bréchet found that after rapid heating during aging there was a decrease in peak hardening. Another study by Deschamps and Nicolas [9] showed that with rapid heating of Al-Zn-Mg, particles become unstable and dissolve. This results in variations in average grain size since the small particles dissolve much more quickly than larger particles. Deschamps et al. [10] found that after rapid heating during aging the initial precipitate radius is larger than after slow heating. Nucleation of η′ is difficult in the rapid heating because of the reversion of GP zones [10].

This paper investigates the effects of heating rates on two 7000 series aluminum alloys using a test which was developed to obtain a distribution of heating rates throughout a single specimen, similar to that of the Jominy end quench test [11]. Tests were conducted with variable heating rates during both solution and aging treatments.

Experimental

The effects of heating rate were studied on two wrought aluminum alloys, AA7136 which contains Zr as the dispersoid and AA7075 which contains Cr as the dispersoid, the latter being much more quench sensitive (Fig. 1).

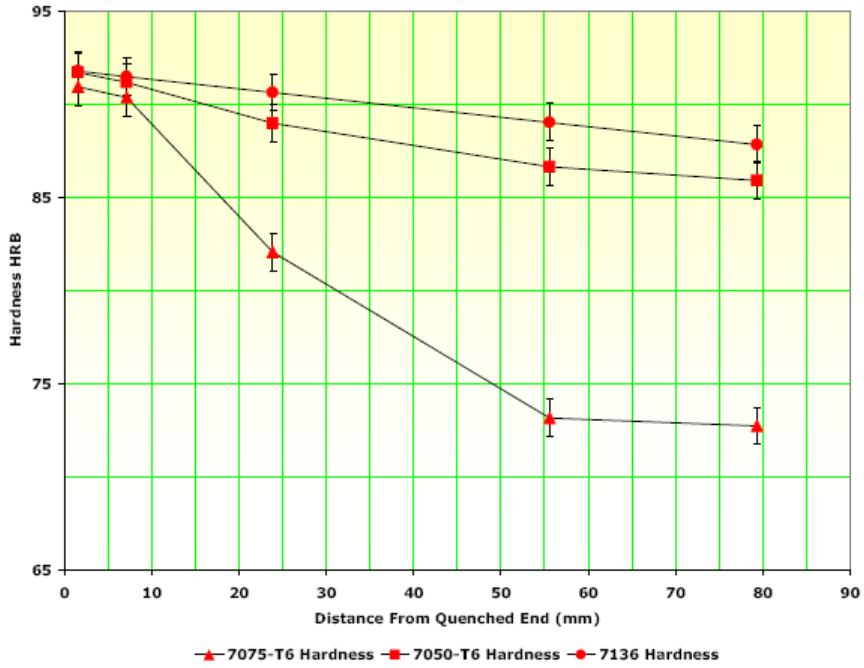

Figure 1: Quench sensitivity of selected 7000 alloys [12]

A test was developed similar to the Jominy end quench test, ASTM A255, where instead of one dimensional cooling, there is one dimensional heating. A schematic of the apparatus constructed for this test is shown in Figure 2. It consists of a potassium nitrate 50% and sodium nitrate 50% salt bath which is placed in a conventional furnace. The top of the furnace is insulated except for an approximately 2.54 cm diameter hole which fits the standard Jominy bar. While conducting the test the bar was hung so that it sat about 2.54 cm in the molten salt. The bar was then covered with insulating material in order to promote the one dimensional heating of the bar. Temperatures were recorded at 1.3 cm from the end of the bar in the salt, 3.8 cm, and 7.6 cm using K type thermocouples and an Omega 3000 series datalogger. The time constant of the thermocouples is about 0.003 s and since data was collected every 1 s, the time constant is insignificant. The test matrix for this type of "reverse" Jominy test, which will be referred to as RJ, is presented in

Table 1.

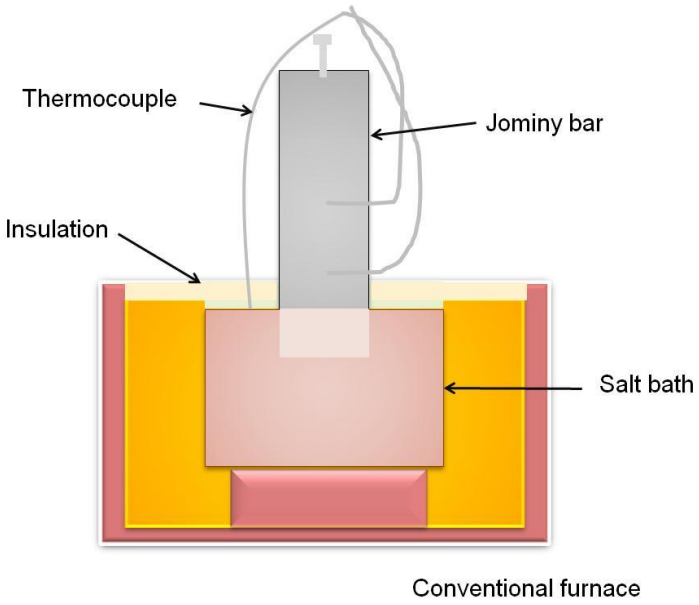

Figure 2: Schematic of reverse Jominy apparatus

Table 1: Test Matrix

	Solution Heat Treatment	**Age Heat Treatment**
7136	Reverse Jominy 475C, 24hr	Conventional Furnace 121C, 24hr
7136	Reverse Jominy 475C, 24hr	Conventional Furnace 250C, 2hr
7136	Conventional Furnace 475C, 24hr	Reverse Jominy 250C, 2hr
7075	Reverse Jominy 480C, 24hr	Conventional Furnace 121C, 24hr
7075	Reverse Jominy 480C, 24hr	Conventional Furnace 250C, 2hr
7075	Conventional Furnace 480C, 24hr	Reverse Jominy 250, 2hr

Hardness profiles were obtained using the Rockwell B scale on a Wilson digital Rockwell tester. Four flats were milled 0.381 mm from the surface on each RJ bar. Hardness measurements were taken every 3.17 mm.

In addition to the RJ tests, samples of each alloy were cut, 2.54 cm diameter, and 0.635 cm thick. One sample of each alloy was solutionized by complete immersion into the same salt bath used for the RJ tests for five hours and one sample was solutionized with a conventional air furnace for five hours. Both were aged using the common industrial T6

aging treatment, 121C for 24 hours [13]. Hardness measurements were taken on these samples after aging.

Optical and SEM microscopy was used to investigate differences in microstructures after various heating rates.

Results and Discussion

Time-Temperature Data

Figure 3 presents the time temperature data at a point submerged in salt, 12.7mm from the end of the bar and a point 12.7mm above the salt of an AA7136 bar and an AA7075 bar solutionized using the RJ method. At the point 12.7 mm above the salt, the maximum heating rate for AA7136 was about 23^{o}C/s and 12.7mm above the salt the maximum heating rate was about 12^{o}C/s. The maximum heating rates for AA7075 were 14 ^{o}C/s and 9 ^{o}C/s at 12.7mm from the bottom and 12.7mm above the salt, respectively. The heating rates versus time and temperature are presented in Figure 4. Figures 5 and 6 show the effects of heating rate during aging. Maximum heating rates during aging of AA7136 and AA7075 were about 3.7^{o}C/s at 12.7mm and 2-2.5^{o}C/s at 12.7mm above the salt for both alloys.

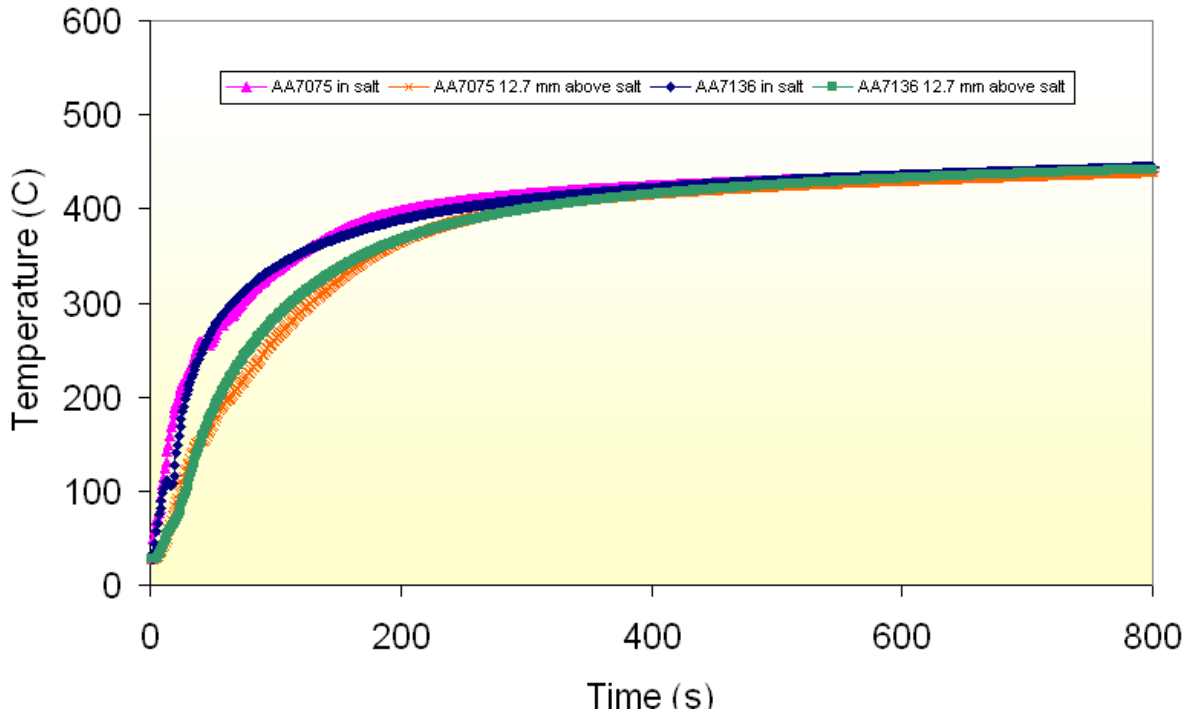

Figure 3: Time-temperature data for RJ during solution treatment

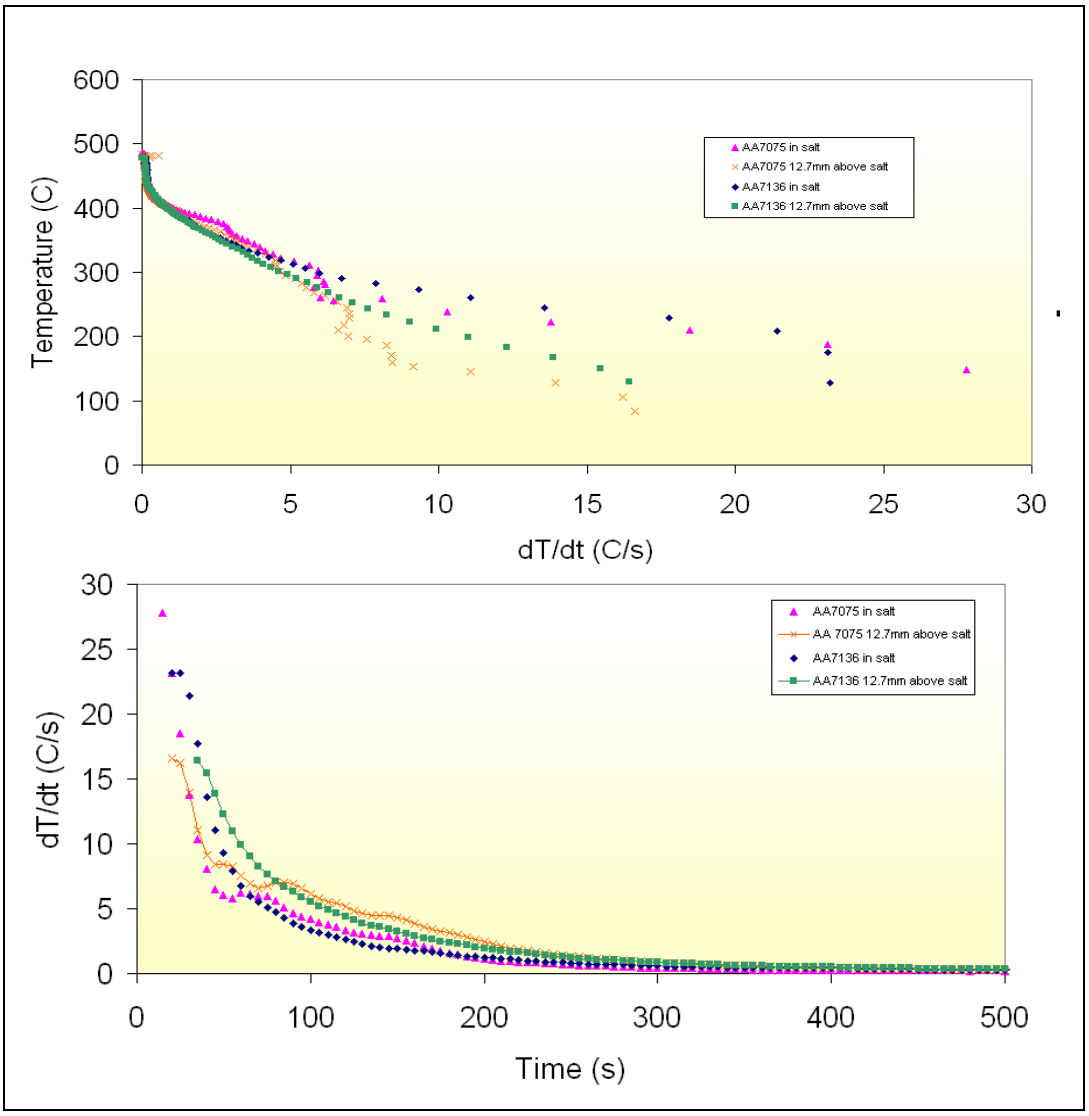

Figure 4: Heating rate versus time and temperature for RJ during solution treatment

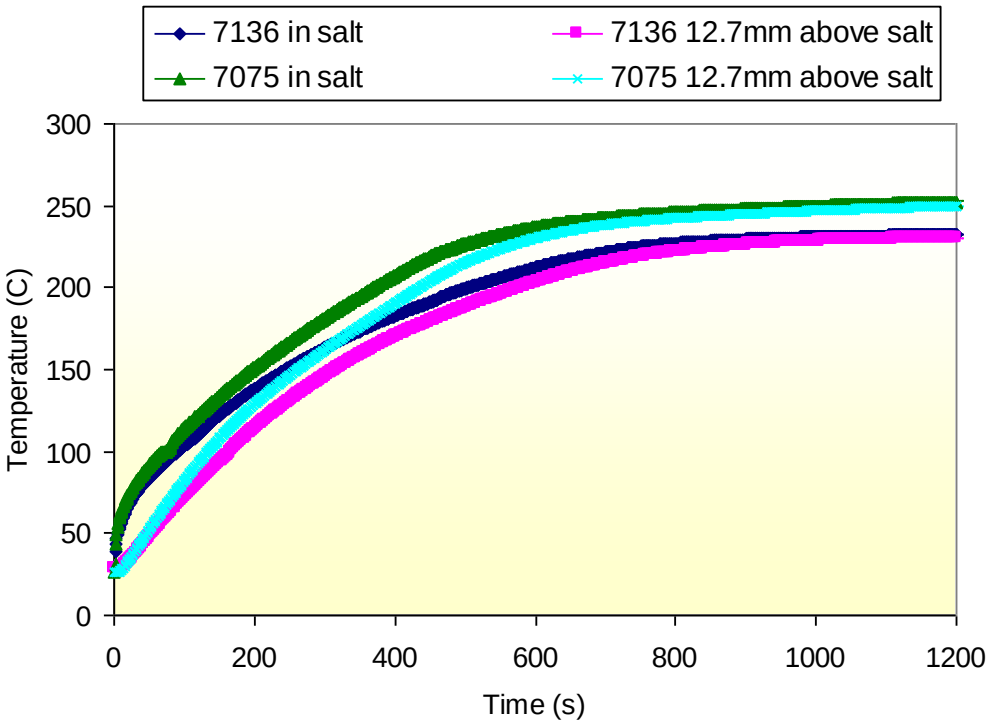

Figure 5: Time-temperature data for RJ during aging treatment of 250°C, 2 h

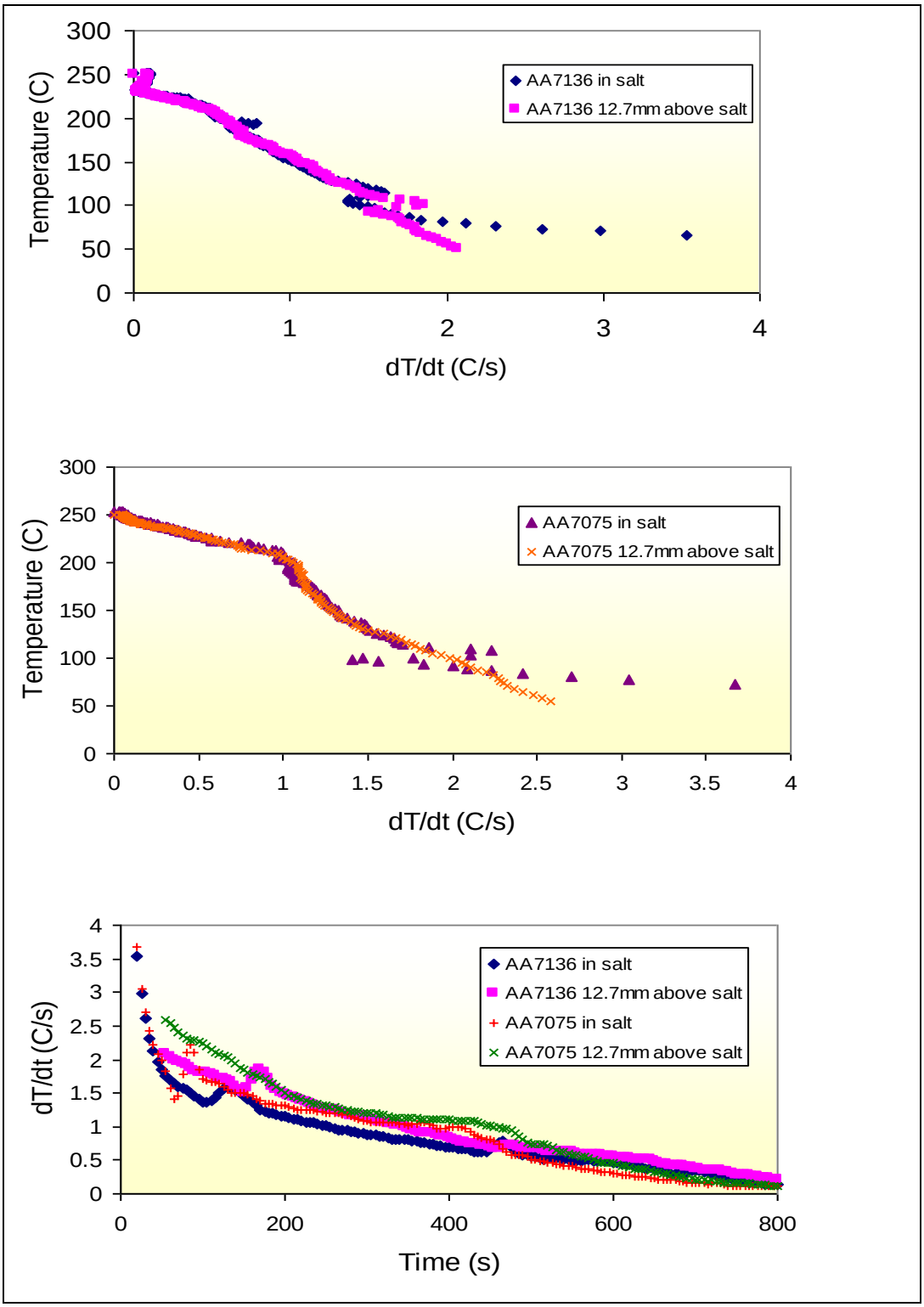

Figure 6: Heating rate versus time and temperature for RJ during aging treatment of 250^{o}C, 2 h

Hardness Data for AA7136 and AA7075

After an AA7136 specimen was solutionized using RJ and aged at T6, 121^{o}C for 24 h, the hardness was slightly higher at the rapidly heated end. There may not be a difference in hardness after solutionizing using RJ and aging at 250^{o}C for 2 h. Figure 7 shows the hardness profile along the bar.

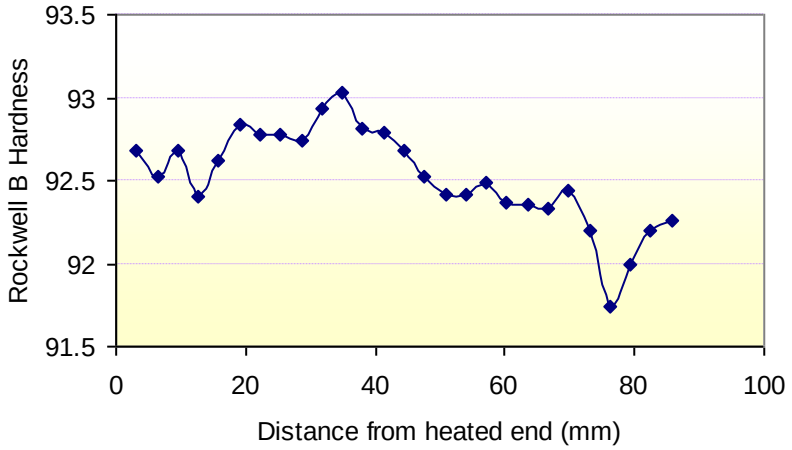

Figure 7: Hardness profile of RJ solution treatment of AA7136-T6

The average hardness for the six measurements closest to the rapidly heated end and the average of the six measurements closest to the slow heated end were calculated for each bar. Figures 8 and 9 present the bars which experienced solutionizing by RJ and Figure 10 presents those bars which were aged by RJ.

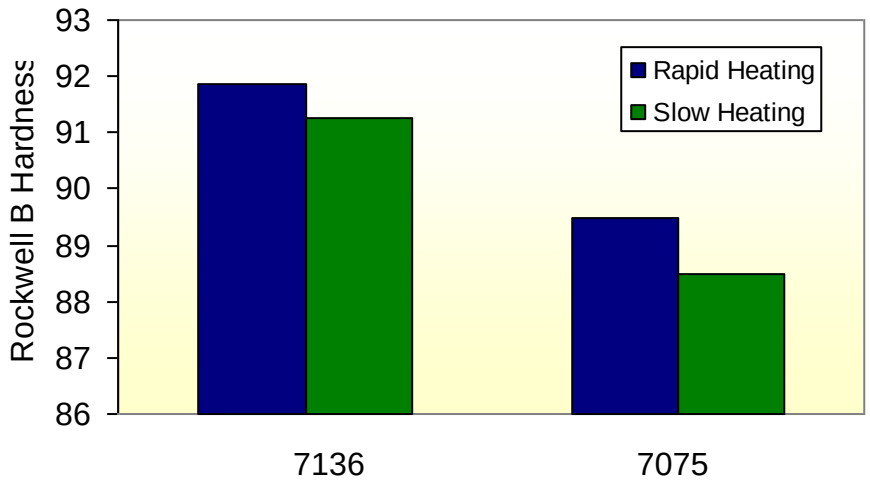

Figure 8: Effects of heating rate during solution treatment with aging at 121^{o}C for 24 hours

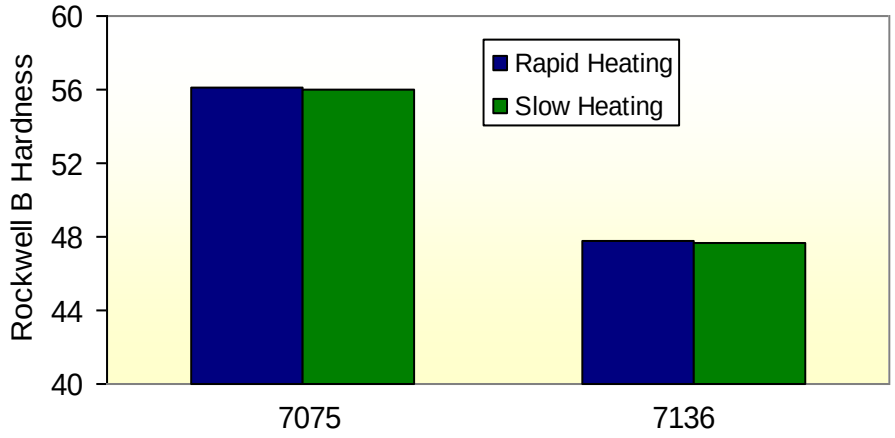

Figure 9: Effects of heating rate during solution treatment with aging at 250^{o}C for 2 hours

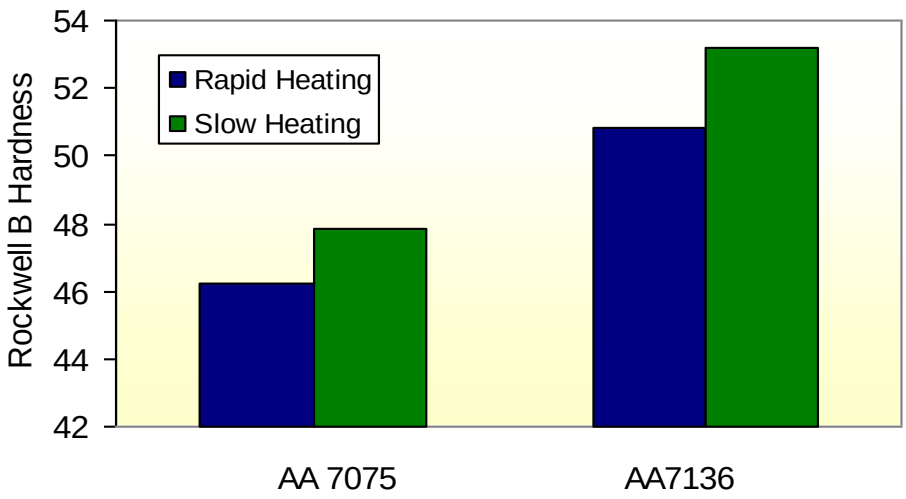

Figure 20

Figure 10: Effects of heating rate during aging treatment

Microstructure

Figures 11 and 12 are SEM images of AA7075 and AA7136 after a salt bath heat up and an air heat up in a furnace, followed by T6 aging treatment. Figures 13 and 14 are optical photomicrographs of the two alloys after RJ during solution treatment followed by a T6 age. The rapidly heated solution treatments result in finer grains. This agrees with the literature [4-7,9,10]. The RJ samples have more equiaxed grains because they were solutionized for longer. The grains are even more equiaxed after rapid heating.

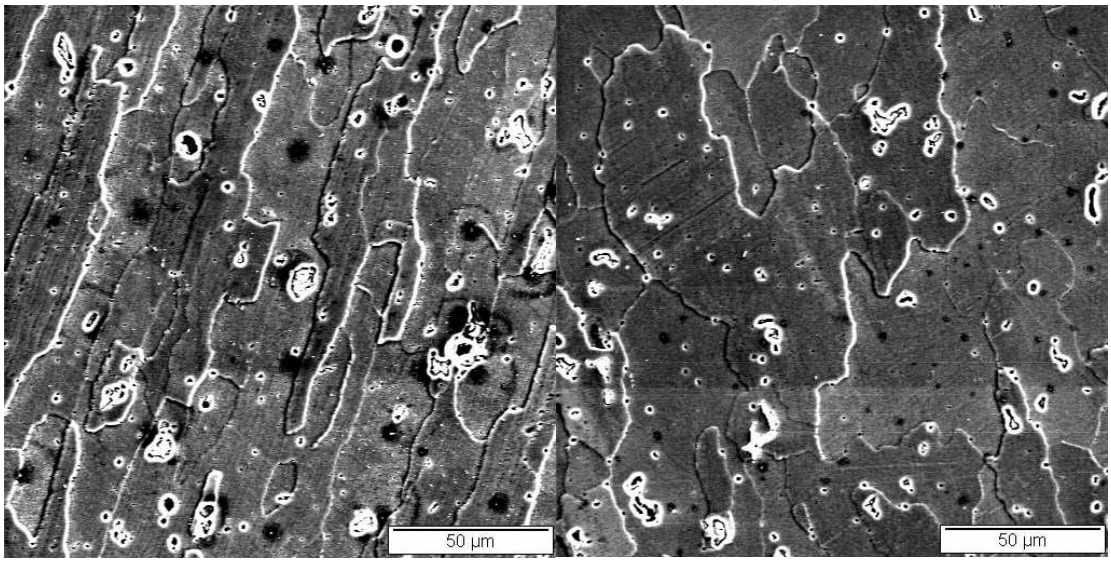

Figure 11: SEM photomicrograph of AA7075-T6 etched with Keller's reagent (left) solution treatment in salt bath (right) solution treatment in air convection furnace

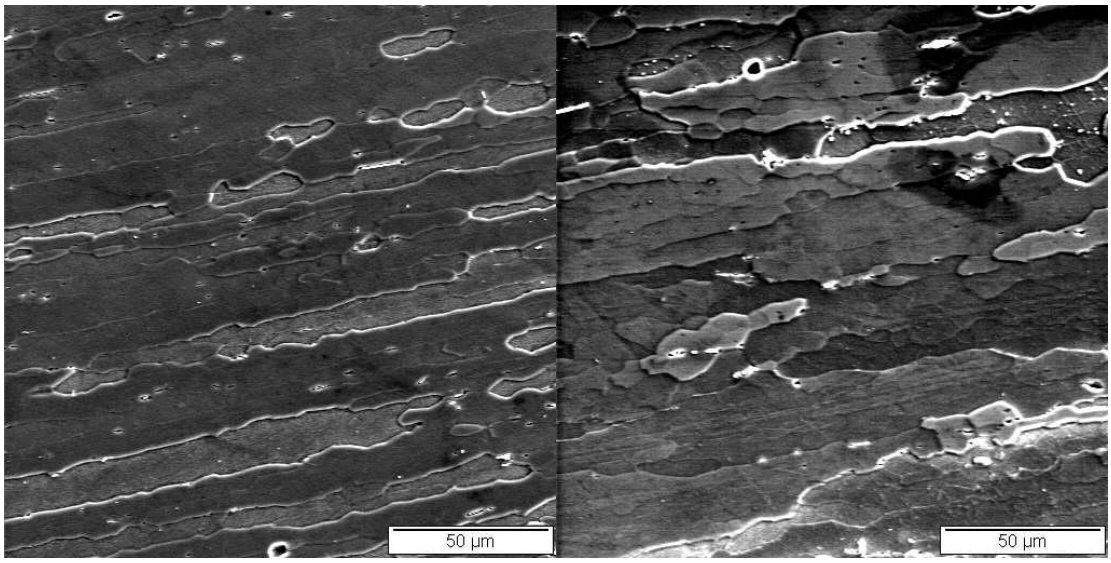

Figure 12: SEM photomicrograph of AA7136-T6 etched with Keller's reagent (left) solution treatment in salt bath (right) solution treatment in air convection furnace

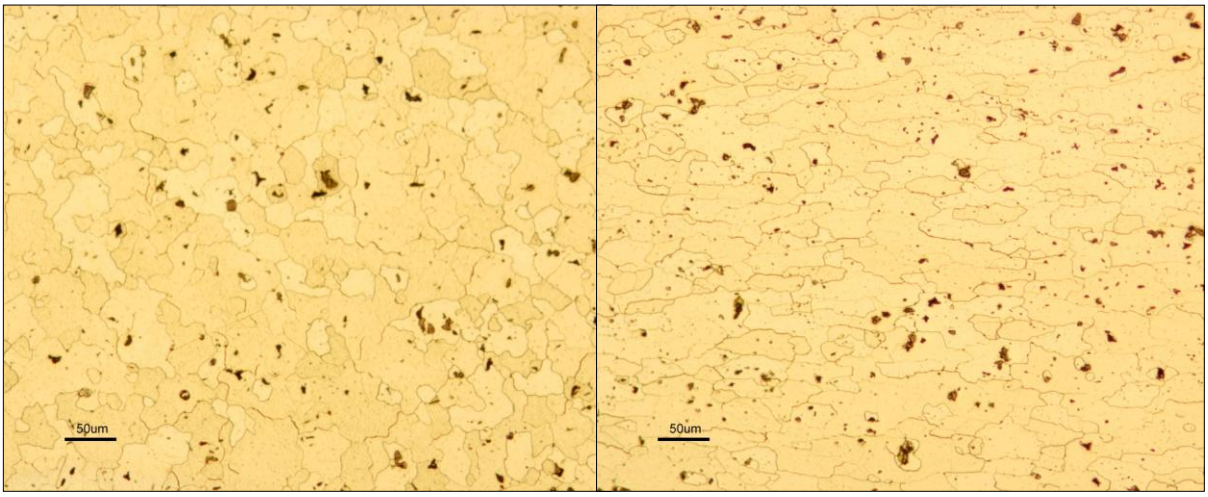

Figure 13: Photomicrograph of AA7075 etched with Keller's reagent, RJ during solution treatment followed by T6 (left) rapidly heated end (right) slow heated end

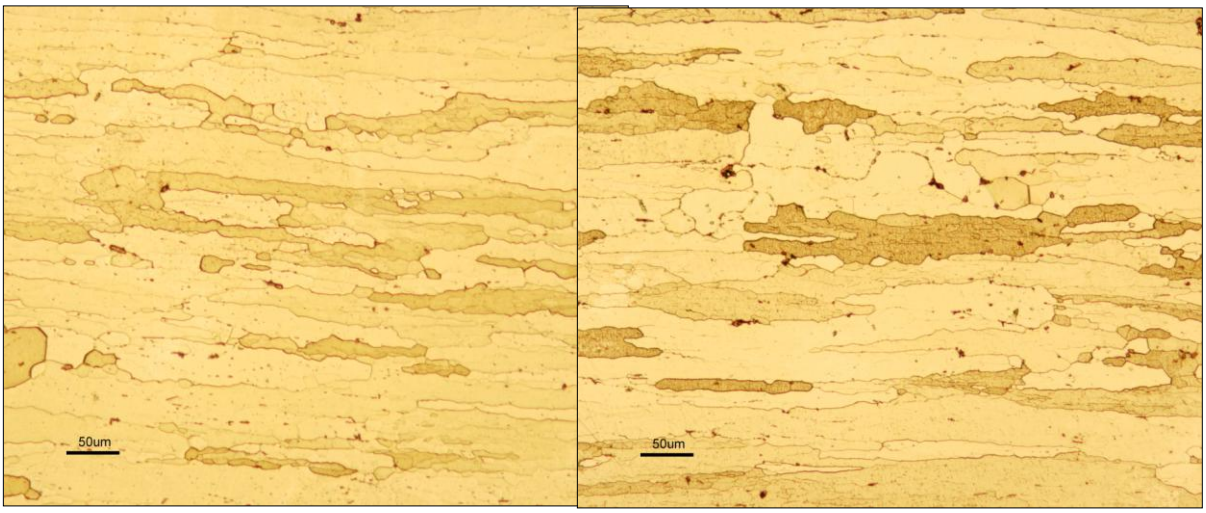

Figure 14: Photomicrograph of AA7136, etched with Keller's reagent, RJ during solution treatment followed by T6 (left) rapidly heated end (right) slow heated end

Future Work

Future work with reverse Jominy testing should include a test on the heating rates during T6 aging using an oil bath; since the salt bath was not molten at 121^{o}C, only the aging temperature of 250^{o}C was studied in this paper. This research should also be modeled in

order to predict properties similarly to Quench Factor Analysis, which has been conducted on a number of aluminum alloys during a regular Jominy end quench test [14, 15].

Summary

A test was developed in order to determine the effects of heating rate. It was found that rapid heating during solutionizing results in a harder, finer microstructure, while rapid heating during aging will result in a softer microstructure, probably due to the reversion of GP zones [10].

Bibliography

1. V.T. Zaspalis, S. Sklari, M. Kolenbrander, The effect of heating rate on the microstructure and properties of high magnetic permeability MnZn-ferrites, *Journal of Magnetism and Magnetic Materials* 310 (2007) 28-36
2. X. Peng, J. Fan, Y. Yang, Y. Chen, Y. Yin, Investigations to the effect of heating-rate on the thermomechanical properties of aluminum alloy LY12, *International Journal of Solids and Structures* 40 (2003) 7385-7397
3. X. Peng, X. Zhang, J. Fan, B. Chen, Effect of heating-rate on the thermomechanical behavior of aluminum alloy LY12 and a phenomenological description, *International Journal of Solids and Structures* 43 (2006) 3527-3541
4. W.C. Liu, A. Li, C.-S. Man, Effect of heating rate on the microstructure and texture of continuous cast AA 3105 aluminum alloy, *Materials Science & Engineering A* (2007), doi:10.1016/j.msea.2007.05.107
5. C.A. Blue, V.K. Sikka, E.K. Ohriner, P.G. Engleman, G.F. Mochnal, A. Underys, W-T. Wu, M.C. Maguire and R. Mayer, *Infrared Heating of Forging Billets and Dies*, UT-Batelle, LLC
6. P. Kadolkar, H. Lu, C. Blue, T. Ando, R. Mayer, Application of rapid infrared heating to aluminum forgings, *25th Forging Industry Technical Conference*, Detroit, MI (2004)
7. S.S. Sahay, K.B. Joshi, Heating rate effects during non-isothermal annealing of AIK steel, *Journal of Materials Engineering and Performance* 12 (2003) 157-16
8. A. Deschamps, Y. Bréchet, Influence of quench and heating rates on the ageing response of an Al-Zn-Mg-(Zr) alloy, *Materials Science and Engineering* A251 (1998) 200-20739.
9. M. Nicolas, A. Deschamps, Characterisation and modeling of precipitate evolution in an Al-Zn-Mg alloy during non-isothermal heat treatments, *Acta Materialia* 51 (2003) 6077-6094
10. A. Deschamps, F. Livet, Y. Bréchet, Influence of predeformation on ageing in an Al-Zn-Mg alloy—I. Microstructure evolution and mechanical properties, *Acta Materialia* 47 no. 1 (1999) 281-292

11. ASTM A255, *Standard Test Method for Determining the Hardenability of Steel*, ASTM, (2007)
12. D.S. Mackenzie, Private Communication, *Quench Sensitivity of 7136 Aluminum*, Houghton International Inc., Valley Forge, PA, (2007)
13. J.W. Bray, *ASM Handbook Vol. 2*, 29-122, ASM International, Materials Park, OH (1990)
14. D.S. Mackenzie, *Quench Rate and Aging Effects in Al-Zn-Mg-Cu Aluminum Alloys*, PhD Dissertation, University of Missouri-Rolla (2000)
15. S. Ma, M. Maniruzzaman, D.S. MacKenzie and R.D. Sisson, Jr. *A Methodology to Predict the Effects of Quench Rates on Mechanical Properties of Cast Aluminum Alloys*, accepted for publication in Met. Trans B, (2007)

Recommended Future work

Further studies should be done on both the quench sensitivity investigation and reverse Jominy testing.

- TEM should be used to identify the precipitates that form in AA7136 to provide a better understanding of aging kinetics.
- More aging experiments should be conducted to determine the behavior of the alloy under various conditions.
- Different heating methods should be investigated using reverse Jominy, such as using an oil bath so that heating rates during aging can be studied at low temperatures, such as 121^{o}C, the T6 aging temperature for most 7000 series alloys.
- The effects of a very slow heating rate, such as less than 1^{o}C/s should be studied as well.
- The relationship between heating rate and resultant properties should be modeled similarly to Quench Factor Analysis. This could allow for property prediction after various heating rates.

Conclusions

The purpose of this study was to determine the quench sensitivity of a new alloy, AA7136, and to develop a test method to determine the effects of heating rate. This research presents the quench and heating rate sensitivities of 7000 series aluminum alloys. It was found through Jominy end quench tests that the alloy AA7136 is not quench sensitive. Rockwell B hardness measurements were taken in order to relate the strength to cooling rate. The hardness varied by less than 5 HRB along the Jominy end quench bar indicating that the alloy is not strongly affected by cooling rate. Since AA7136 is not quench sensitive, this alloy may be made into thick plates without compromising strength in the center of the part after a slow cool.

There is no current standard for an experiment to study the effects of heating rate like there is for cooling rate (JEQ). A reverse Jominy heating test was successfully developed which results in a distribution of cooling rates throughout the bar. Experiments where the heating rate was varied during solution treatments and aging treatments were applied to standard Jominy end quench bars of AA7136 and AA7075. Optical and SEM microscopy was used to study the microstructural differences between a fast and a slow heating rate. Rapid heating during solutionizing led to a fine, equiaxed grain structure. Hardness was related to heating rate. It was also found that rapid heating during solutionizing led to a slightly harder microstructure, although the hardness values varied by less than 2 HRB. This can be attributed to the finer microstructure after increased heating rates. Rapid heating during aging, however, resulted in a softer microstructure. This phenomenon can be attributed to the lack of GP II zones, which the hardening phase η´ precipitates on. GP

zones grow at lower temperature than the aging temperature tested, 250^{o}C, and the slower heating rate allowed enough time at lower temperatures for the GP zones to form.